

Finite Temperature Dynamics of Spin Solitons with Applications in Thermocouples and Refrigerators

Chaofan Gong^{ID 1}

¹*waiting for revisions*

The exploitation of spin Berry phases to generate emergent fields for producing miniaturized and high-quality inductors has enjoyed considerable popularity among proponents of quantum technologies [[Nature 586, 202 \(2020\)](#)]. Inspired by this breakthrough, we extend its mechanism to spin thermoelectrics by probing responses of ferrimagnetic domain walls (DWs) to thermal gradients. Similarly, voltages here stem from DW-spin collective motion, in contrast to normal electron transport phenomena. We further develop finite-temperature dynamics to investigate thermoelectric figures of merit and attribute corresponding quantum superiority to ultrafast spin evolution of ferrimagnetism with tunable non-Abelian phases. We propose a more likely cause of DW motion towards hot or cold regions (contrary to conclusions of previous reports) and verify existence of efficient magnon-momentum transfers. These findings deepen our understanding of heat-driven DW kinetics and suggest profitable new directions in an emerging realm of spincalortronics.

Introductions. After-heat in our life is ubiquitous. It occurs in human bodies, industrial products, solar beams, electronic components, and geothermal collections. Heat is the most widely existing form of energy, and our domestic electricity mainly comes from thermal power generation. Conventional thermocouples utilize Seebeck, Nernst, and Thomson effects to convert waste heat into electricity, and we can also conversely harness Peltier effects for refrigeration. As Moore's law reaches saturation, these thermoelectric elements are encountering significant obstacles, shifting our attention to their quantum counterparts. In quantum physics, spins are excellent candidates, and they have been utilized with striking success in memories [[1](#)] and computations [[2](#)].

Recently, the further revolution [[3](#)] in which spin Berry phases are used to generate electromagnetic fields has enabled inductors to be fabricated, and these quantum inductors are surprisingly effective even above room temperature [[4](#)]. It has also been discovered that large Berry curvature in magnetic semi-metals [[5](#)] and antiferromagnets [[6–11](#)] will enhance thermoelectric transports, indicating that combinations of spins and thermoelectronics are becoming new trends [[12–15](#)]. When spins condense into various textures, their Berry phases will form scattering potentials hindering heat transport [[16](#)], thus effectively improving thermoelectric figures of merit. These results all testify remarkable efficiency of spin emergent fields, and making full use of this emergent electromagnetism to design advanced topology-quantum-materials [[17](#)] is a grand challenge [[18](#)] in the realm of contemporary science-technology, inspiring us to employ thermal gradients to excite these fields for inducing electricity. Intuitively, thermal gradients will stimulate magnon flows (i.e. spin Seebeck and Nernst effects [[19, 20](#)]) and entropy increases [[21](#)], boosting spin collective motion to make Berry phases (serving as "magnetic vector potential") change with spacetime to generate spin-motive force for power generation.

Thermal gradients furnish driving methods which are more productive [[22, 23](#)], convenient [[24](#)], and low-loss [[19](#)] than currents and magnetic fields, leading to pollution-free and recyclable spincalortronics [[25](#)]. Meanwhile, thermal gradients also offer very effective ways for producing [[26](#)] and stabilizing [[27](#)] DWs. Beyond applications in spin batteries [[28](#)], heat-driven DW dynamics can realize green refrigerators [[29–31](#)], chaos generators [[32](#)], and random-number devices [[33](#)]. Compared with techniques of magnetic susceptibilities, neutron scatterings, and magneto-optical micro-

scopes, thermal transport measurements can detect magnetic orders more operatively, especially for antiferromagnetism [[34–36](#)] without net magnetic moments.

To deepen our understanding of responses of DWs to thermal gradients, we naturally choose ferrimagnets with Dzyaloshinskii-Moriya interactions (DMIs). Ferrimagnets have advantages in strong quantum fluctuations [[37](#)], long spin-coherence lengths [[38](#)], low damping factors [[39](#)], tunable spin densities [[40](#)], high electrical sensitivities [[41](#)], and enormous emergent fields [[42, 43](#)]. DMIs preferably suppress the degree of freedom of DW precession [[44, 45](#)] and expedite Zeeman couplings and spin stagger [[46](#)], benefitting translational motion to attain ultrafast spin dynamics [[47](#)] so that relativistic effects [[48](#)] cannot be bypassed. These phenomena essentially originate from ferrimagnetic non-Abelian Berry phases [[49](#)] producing extra spin nutation [[50](#)], in contrast to ferromagnetic Abelian phases.

Nevertheless, under thermal gradients, physical mechanisms behind Berry-phase-dominated DW dynamics still remain elusive. As mentioned in Ref. [[51](#)], it is unclear what forces are exerted on DWs, and what is the predominant factor that causes DWs to move to hot or cold regions. Recent experiments observe that ferromagnetic DWs can move to hot [[52–56](#)] or cold [[26, 56–58](#)] regions, individually attributed to magnon spin torque [[56, 59](#)] or magnon momentum transfers [[57](#)]/ thermal diffusion [[26, 56](#)]/ Nernst-Ettingshausen effects [[58](#)] (DWs we refer to here include skyrmions as well). We perceive that these conclusions are not complete because they not quantitatively analyze various factors and neglect entropy-increase processes [[60–62](#)] that have significant impacts on DW velocities. DW entropy relates to Heisenberg interactions [[60, 63–68](#)], DMIs [[69–71](#)], anisotropy interactions [[62, 72, 73](#)], and Zeeman couplings [[21](#)] and can promote DW migration towards hot or cold ends depending on positive or negative signs of the above interactions. In addition, thermal gradients will stimulate excessive dipole fields [[74](#)], making ferromagnetic DWs move to hot regions. Here we revisit these problems in ferrimagnetism generalized to ferromagnetism and antiferromagnetism and conclude DW migration to hot regions in other experiments due primarily not to magnon spin-transfer torque but to entropy and Dzyaloshinskii-Moriya [[75](#)] vector potential.

On the other hand, interactions between magnons and DWs also need to be solved. Several articles in Refs. [[29, 59, 66, 76–79](#)] assume that DWs are non-scattering solitons having fully-transmitted Pöschl-Teller potential [[80](#)].

A small number of reports think that wide DWs [68] and high-frequency magnons [68, 81] are conducive to scatterings. Quite a few papers ruminate that narrow DWs and low-frequency magnons will have noticeable reflection [16, 45, 82–110] and even inelastic scatterings [111] and resonances [81, 91, 92, 94, 112–116], and Refs. [91, 117] further claim that scatterings will provoke the strongest momentum transfer when magnon wavelengths are close to DW widths. From our viewpoint, various factors (comprising DW configurations [16, 84, 85, 87, 90, 113, 118], magnon polarization [83, 86, 106], temperature, magnetic fields [93], exchange interactions, DMIs [45, 83, 87, 88, 116, 118–121], easy [88, 93, 95, 116] & hard [83, 88, 104, 112] axis anisotropy, damping [105], and pinning [79]) affecting interactions between magnons and DWs can be attributed to Lagrangian alterations that vary DW potential and magnon frequencies to affect scatterings, providing intuitive-overall comprehension for magnon-DW interactions and demonstrating that DWs are excellent magnon regulators. This permits us to better devise logic-gates [107, 122], filters [84, 85], polarizers [86], phase-retarders [123], fibers [124], interferers [78, 125], Stern-Gerlach generators [120], Goos-Hänchen producers [126, 127], and focalizers [128] via magnons with the above regulable parameters.

Ultimately, the extrapolation [63] that ferrimagnetic DWs migrate to hot ends below Walker-breakdown limits and above angular-momentum compensation points (in other circumstances, they shift to cold ends) is also incomplete because it dismisses substantial momentum transfers so as to engender anomalous divergence of physical quantities owing to exploiting zero-temperature equations to dissect finite-temperature cases [129–132]. Ref. [63] recognizes that magnons are entirely transmissive, but it misses a essential that magnons will transmit momentum via redshifts [133] after passing through DWs apart from angular-momentum transfers. We demonstrate in this study that mutual scatterings of magnons and emergent fields is sufficiently robust to make DWs overcome entropy forces and migrate to cold ends. By considering influences of various forces on DW, we can forecast their behaviors more accurately, avoiding information losses that DW velocities are slowed down or even reversed due to environmental heat.

Finite-temperature dynamics dominated by Berry phases. Thermal gradients will excite magnons and electrons [Fig. 2(a)]. Magnons exert spin-angular-momentum and momentum to DWs, while electrons impart angular momentum to DWs by spin transfer torque and spin orbit torque (here electron momentum transfers [134] are very small [135]). Under thermal gradients, even accounting for charge pumping [136], DW velocities caused by magnons are much larger ($\sim 10^3$) than that of electron spin-transfer torque [55, 57, 137]. Due to the existence of the non-magnetic metal layer Pt in our experiment, electrons also have spin-orbit torque, which is two times (proportional to ratios of DW widths to film thicknesses [138]) greater than spin-transfer torque but still less than magnon influences (spin-orbit torque likewise enhance magnon propagations [139]). In the experiment, we apply a current $1 \times 10^9 \text{ A} \cdot \text{m}^{-2}$ corresponding to a thermal gradient $1 \times 10^7 \text{ K} \cdot \text{m}^{-1}$ (Seebeck effects), and DWs can not overcome pinning to start moving. However, in insulators [52, 53] where only magnons are present, DW motion is observed with a small thermal gradient $\sim 1 \times 10^3 \text{ K} \cdot \text{m}^{-1}$. These experimental phenomena

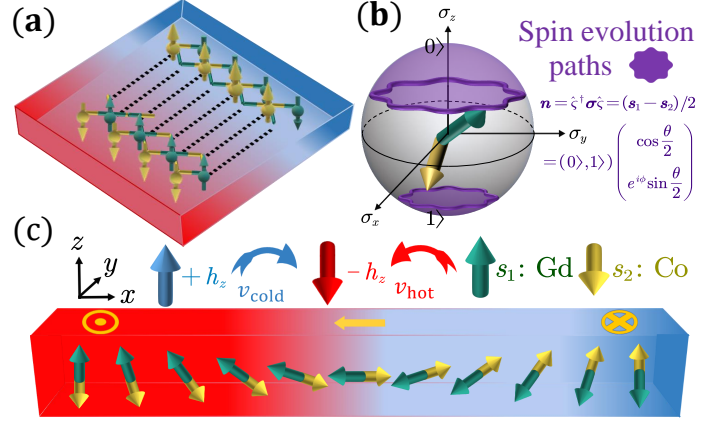


FIG. 1. (a) Thermal gradients excite magnon flows in a ferrimagnetism composed by Co and Gd. (b) Spin staggering evolution on a Bloch sphere constitutes non-Abelian Berry phases. (c) Left-handed Néel DWs (topological charges equal one, i.e. $q = 1$) driven by magnon spin torque, magnon momentum transfers, magnetic fields, and thermodynamic entropy forces can move to hot or cold regions under different parameters.

further show that electron flows excited by thermal gradients are inoperative in DW motion. Additionally, thermal diffusion here is ineffective on account of a large cross-sectional area [140].

Synthesizing the above analysis, we consider the magnon adiabatic and diabatic spin torque Ω_s and β_s , magnon redshift β_r , magnon momentum transfer β_R , entropy effect β_T , vertical magnetic field h_z , antiferromagnetic-coupling exchange interaction ϵ_{ne} , DMI ϵ_{dm} , easy axis anisotropy ϵ_{an} , hard axis anisotropy $\epsilon_{ah}(m)$ including the thermally induced dipole interaction $\epsilon_{dip}(m)$, and pinning potential \hat{V}_p and compose the DW Lagrangian (the dimension is J) by a spinor [141] [Fig. 2(b)] $\hat{\zeta}_j^\dagger = \left(e^{-i\phi_j} \cos \frac{\theta_j}{2}, \sin \frac{\theta_j}{2} \right)$ (since the spin s_j of each lattice point j is quantized so that (θ_j, ϕ_j) can only take a series of discrete values, for concision, we will adopt Einstein's summation convention to omit these subscripts):

$$\begin{aligned} \hat{\mathcal{L}}_w = & \rho_n n |\hat{\zeta}^\dagger (-i\partial_\tau - \mathcal{J}_m) \hat{\zeta}|^2 + 2n\hat{\zeta}^\dagger (-i\rho_s \partial_\tau - \mathcal{J}_m) \hat{\zeta} - \\ & 2\epsilon_{ne} |a(-i\nabla - \mathcal{A}_r) \hat{\zeta}|^2 + \frac{a^2}{2} (\epsilon_{an} - |\zeta|)[1 - (\hat{\zeta}^\dagger \sigma_z \hat{\zeta})^2] \\ & - (\epsilon_{ah} + \epsilon_{dip}) a^2 (\hat{\zeta}^\dagger \sigma_x \hat{\zeta})^2 + nm h_z \hat{\zeta}^\dagger \sigma_z \hat{\zeta} + \hat{V}_p \end{aligned} \quad (1)$$

with the dynamic coupling $\mathcal{J}_m = (1 - \mathcal{R}) \rho_s \Omega_s - [(1 - \mathcal{R})(\beta_s - \beta_r) - \mathcal{R}\beta_R + \beta_T] \hat{\zeta}^\dagger \sigma \hat{\zeta} \times (\mathbf{j}_m/\hbar) \cdot (\nabla - \frac{\epsilon_{dm}}{\epsilon_{ne}} \mathbf{e}_i)$ between magnons and Berry phases, magnon reflectivity \mathcal{R} , relative spin density $\rho_s = s/n$, polar/azimuth angle θ/ϕ , Pauli matrix $\sigma = (\sigma_x, \sigma_y, \sigma_z)$, magnon current \mathbf{j}_m , reduced Planck constant \hbar , unit vector $\mathbf{e}_i = (e_x, e_y, e_z)$, spin inertia $\rho_n = n/\epsilon_{ne}$, Néel vector $\mathbf{n} = (s_1 - s_2)/2 = \hat{\zeta}^\dagger \sigma \hat{\zeta}$, Co/Gd spin vector s_1/s_2 , net spin density $\mathbf{s} = \mathbf{s}_1 + \mathbf{s}_2$, Co/Gd magnetization M_1/M_2 , vector lengths n and s , time scale τ , lattice constant a , DW Berry phase $\mathcal{A}_\mu = (\mathcal{A}_\tau, \mathcal{A}_r) = (-i\rho_s \hat{\zeta}^\dagger \partial_\tau \hat{\zeta} - \rho_n (\hat{\zeta}^\dagger \partial_\tau \hat{\zeta})^2, -i\rho_s \hat{\zeta}^\dagger \partial_r \hat{\zeta} - i\zeta \sigma)$, relative net magnetization $m = (\gamma_1 s_1 - \gamma_2 s_2)/\nu n$, Co/Gd gyromagnetic ratio γ_1/γ_2 , vacuum permeability ν , and DMI characteristic scale $\zeta = \epsilon_{dm}/\epsilon_{ne}$. The above interactions result in left-handed Néel DWs [Fig. 2(c)], and their dynamic processes under magnons are shown in Figs. 3(a)-(c).

$\hat{\zeta}^\dagger$ and $\hat{\zeta}$ represent DW creation and annihilation operators with the number $N = \hat{\zeta}^\dagger \hat{\zeta}$ of DWs. Other advantages of expressing Eq. (1) by spinors are that

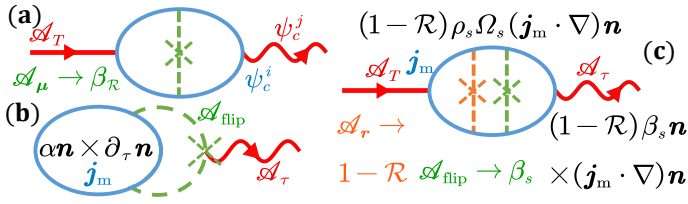


FIG. 2. (a) Temperature-gradient (equivalent to a thermal vector potential \mathcal{A}_T) excited magnons are reflected (β_R) by the DW Berry phase \mathcal{A}_μ . Considering more general inelastic scatterings, magnon incident (ψ_c^i) and reflective (ψ_c^j) states are different. (b) The spin flip scattering $\mathcal{A}_{\text{flip}}$ produces the lateral damping α , hindering a time-dependent variation \mathcal{A}_τ of Berry phases motivated by a magnon flow j_m . (c) When magnons interacting with an emergent field \mathcal{A}_r pass through $(1 - \mathcal{R})$ DWs, spin torque including adiabatic and diabatic terms is produced, in which the diabatic term β_s also comes from the spin flip scattering $\mathcal{A}_{\text{flip}}$.

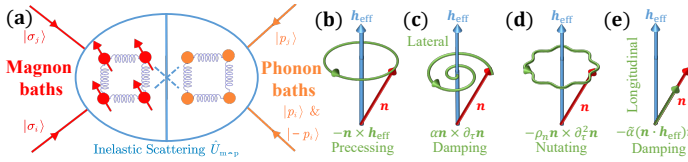


FIG. 3. Magnon and phonon thermal baths at finite temperature will induce non-Markov and Markov friction (a), making spin evolution have extra longitudinal damping (e) in addition to precession (b), lateral damping (c), and nutation (d). The motion (d) is the embodiment of ferrimagnetic non-Abelian phases, which does not exist in ferromagnetism. The motion (e) causes magnetization to decrease with temperature and is the reason for the existence of Néel and Curie temperature.

they avoid the Berry-phase-evoked uncertainty [142] $2j\pi$ (i.e. $\int_0^\tau \mathcal{A}_\tau d\tau = -\int_0^\tau [i\rho_s \hat{\sigma}^\dagger \partial_\tau \hat{\sigma} + \rho_n (\hat{\sigma}^\dagger \partial_\tau \hat{\sigma})^2] d\tau = -i\rho_s [\phi(\tau) - \phi(0) + 2j\pi] + \dots$ with the integer j) and non-physical phenomenon that Lagrangian relies on choices [143] of gauge potential. The first term in $\hat{\mathcal{L}}_w$ signifies spin nutation [50] bringing about DW mass and ultrafast dynamics [Fig. 4(d)].

At the finite temperature T , spins are coupled to phonon-and-magnon thermal baths [Fig. 4(a)], making fluctuation-dissipation terms appear so that magnetization of each lattice point decreases with temperature [144]. The dissipative Lagrangian can be denoted as $\hat{\mathcal{L}}_d = \frac{1}{2}\alpha n \rho_n (\partial_\tau \hat{\sigma}^\dagger \boldsymbol{\sigma} \hat{\sigma} + \hat{\sigma}^\dagger \boldsymbol{\sigma} \partial_\tau \hat{\sigma})^2 + \frac{1}{2}\tilde{\alpha} U_w (\hat{\sigma}^\dagger \boldsymbol{\sigma} \hat{\sigma})^2$ [U_w is the potential energy in Eq. (1)], where the damping parameter α contains the Markov α_p , non-Markov [145] $\int_{-\infty}^\tau [\alpha_m(\tau - \tau')] \frac{\partial \tau'}{\partial \tau} d\tau'$, and DW structure scattering-relation [146–148] $\alpha_0 \sqrt{\epsilon_{ne}/\epsilon_{an}} \mathbf{n} \cdot (\nabla \times \mathbf{n})$ (the strength parameter α_0) parts, and the longitudinal relaxation $\tilde{\alpha}$ evinces spin and magnetization vector lengths decreasing with temperature [144] [Figs. 4(b)–(e)]. Spins in Markov processes are connected to phonons and in Berry-phase-induced non-Markov procedures are linked to magnons, and the homographic energy-fluctuation is $\langle \delta \mathcal{H}(t) \rangle = \int_0^\infty d\omega \frac{\rho_n^2 \hbar \omega \cos(\omega \tau)}{2 \tanh(\hbar \omega / 2k_B T)} [\int_0^\infty d\omega \exp(-\omega \tau) \alpha_m + 4\pi (\alpha_p - \tilde{\alpha})]$ with the magnon frequency ω and Boltzmann constant k_B . These phonon baths will also trigger the longitudinal-spin-length fluctuation $\langle \delta n_{||}(t) \rangle = \int_0^\infty d\omega \frac{\tilde{\alpha} \rho_n \cos(\omega \tau)}{2 \tanh(\hbar \omega / 2k_B T)}$. Atomic spin dynamics simulations [149] also verify these additional friction-damping effects due to temperature.

Entropy forces acting on DWs. To simplify problems, we equate entropy increase efficacy [66] under thermal gradi-

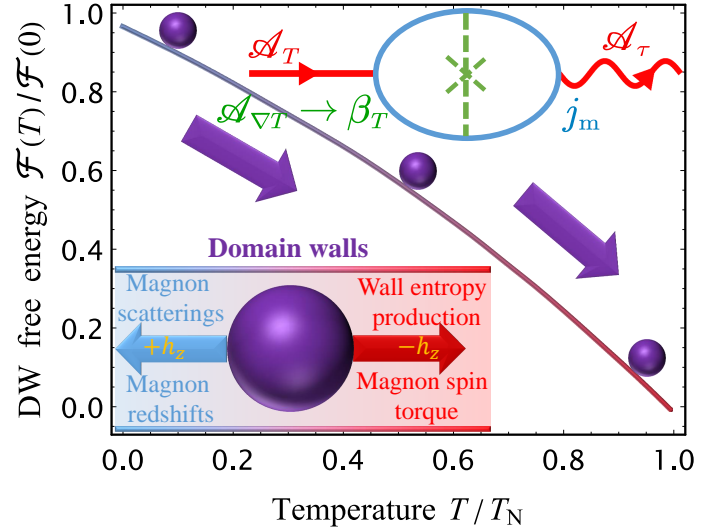


FIG. 4. Of factors affecting DW velocities, entropy forces make DWs move to hot regions, while magnons and magnetic fields can make them move to hot (magnon spin torque and $+h_z$) or cold (magnon scatterings, redshifts, and $-h_z$) ends. Entropy increases are tantamount to free energy reductions, and free energy decreasing with temperature always makes DWs move towards hot regions like playing slides (the Néel temperature is T_N). Here we equate DW entropy generation as a gauge field $\mathcal{A}_{\nabla T}$ and then write it as the diabatic strength parameter β_T in Eqs. (6)–(7).

ents to forces acting on DWs [135], avoiding complexity of dealing with non-equilibrium path integrals. Entropy generation is equivalent to free-energy diminutions, which can be derived from Eq. (1), i.e.

$$\{1 + \alpha [n(T)/n(0)]^2\}^{-1} \Delta \mathcal{F} = 4 \{\epsilon_{ne} [\epsilon_{an} + (\epsilon_{ah} + \epsilon_{dip}) \cos^2 \phi]\}^{1/2} - \pi \epsilon_{dm} \cos \phi + nm h_z/a, \quad (2)$$

and the homologous force $F = \frac{d\mathcal{F}}{dx} = \frac{d\mathcal{F}}{dT} \nabla T$ can be paraphrased as an intensity quantity $\beta_T = -\frac{2h}{nk_B} \frac{\partial \mathcal{F}}{\partial T}$ in diabatic spin torque. For convenience, we unify the thermally induced dipole field $\epsilon_{dip} = \frac{1}{2} \frac{\nu a L_z}{L_z + \Delta} \int \frac{\partial(M_1 - M_2)}{\partial T} \frac{\partial T}{\partial x} dx$ to hard axis anisotropy with the DW with Δ and film thickness L_z . Here these thermodynamic factors always make DWs tend to hot ends since all parameters decrease with temperature [Fig. 5]. This conclusion is also applicable to ferromagnetic and antiferromagnetic systems because their energy ground states can be mapped to each other via $s_j \rightleftharpoons (-1)^j s_j$ so that they have the same thermodynamic feature. The force caused by each interaction (containing the Heisenberg interaction [60, 64, 65, 67], DMI [60, 64, 65, 67], and magnetic anisotropy [61, 70, 71]) in Eq. (2) is appreciable, confirming that thermal gradients are efficient driving methods.

Pinning potential. Pinning comprises both internal and external components. Internal components [150] come from the hard-axis anisotropy ϵ_{ah} & ϵ_{dip} and DMI ϵ_{dm} , while external components [151] originate from the translational and rotational symmetry-breakings stimulated by system disorders [Figs. 6(a)–(b)]. Pining is inherent [152], dilates with film thicknesses [153], mediates Gilbert-damping and diabatic-torque production [154], and can be counterbalanced by magnetic fields along easy axes [58] [Fig. 6(c)]. Internal pinning caused by hard axes will be demonstrated in Eq. (6), and here we delineate the external pinning potential as $\hat{V}_p = \epsilon_{px} \exp(i \frac{2\pi}{\Delta} \hat{\sigma}^\dagger \boldsymbol{\sigma} \cdot \mathbf{r}_i) \delta(\mathbf{r} - \mathbf{r}_i) + \epsilon_{p\phi} \hat{\sigma}^\dagger \boldsymbol{\sigma} \cdot \mathbf{s}_i \delta(\mathbf{r} - \tilde{\mathbf{r}}_i) = \epsilon_{px} (1 - \cos \frac{x}{\Delta}) + \epsilon_{p\phi} (1 - \cos \phi)$ with impu-

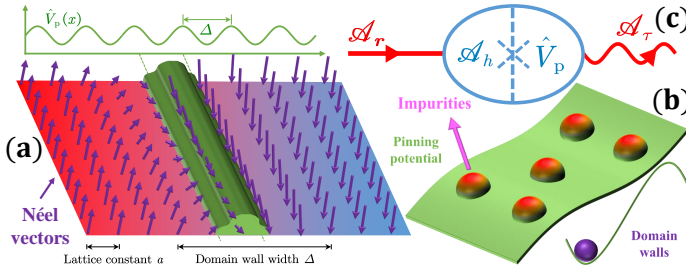


FIG. 5. Impurities break the translational and rotational symmetry of DWs (a), deform DWs (a), and make them move in a periodic potential \hat{V}_p (b). Through quantum tunneling and thermal crawling, DWs cross irregular pinning (a), in much the same way as cars cross speed humps (b). (c) An easy-axis field \mathcal{A}_h can resist pinning and even depin DWs ($\mathcal{A}_r \rightarrow \mathcal{A}_\tau$).

rities impeding translation (elastic impurities: densities $\epsilon_{px} \sim \exp(-\Delta/a)$ and positions r_i) and rotation (magnetic impurities: densities $\epsilon_{p\phi}$, positions \tilde{r}_i , and spins s_i) of DWs. When DW widths approach to characteristic lengths of impurities, pinning is strongest [155]; while Δ is away from these characteristic lengths, broad DWs are more facile to cross pinning [156] owing to the slackly-variable $\sin x/\Delta$ and small ϵ_{px} . Eq. (1) asserts that pinning will diminish DW energy [157], tantamount to curtailing DW widths to enhance magnon reflection [82]. From another perspective, magnetic impurities can correspond to hard-axis anisotropy [see subsequent Eq. (6)], availing magnon reflection by shrinking the DW width $\Delta^2 = \frac{4\epsilon_{ne}(4\epsilon_{an}-\epsilon_{dm}^2/\epsilon_{ne})^{-1}}{1+\epsilon_{ah}\sin^2\phi/[\epsilon_{an}-\nu(M_1-M_2)^2/2]}$. A micromagnetic simulation [88] still visualizes benefit of hard-axis anisotropy to magnon reflection. Elastic external pinning will affect scaling laws and pinning strength in the DW creeping-motion solution (7), while magnetic-external and internal pinning only determines intensity terms (see Ref. [158]).

Interactions between magnons and DWs. For magnons, we regard a spin oscillation $\delta\zeta^\dagger = (\hat{\psi}_\delta^\phi, \hat{\psi}_\delta^\theta)$ and define the magnon two-component field $\hat{\psi}_c^\dagger = (\hat{\psi}_\delta^\theta - i\hat{\psi}_\delta^\phi, \hat{\psi}_\delta^\theta + i\hat{\psi}_\delta^\phi)$, where left ($c = -$) or right ($c = +$) chirality is $\hat{\psi}_l^\dagger = \hat{\psi}_\delta^\theta + i\hat{\psi}_\delta^\phi$ or $\hat{\psi}_r^\dagger = \hat{\psi}_\delta^\theta - i\hat{\psi}_\delta^\phi$ [Fig. 7(a)]. Substituting the above expressions into Eq. (1), we acquire the magnon Lagrangian $\hat{\mathcal{L}}_m = \rho_n n |\hat{\psi}_c^\dagger (-i\partial_\tau - c\mathcal{A}_\tau) \hat{\psi}_c|^2 + 2n\hat{\psi}_c^\dagger (-i\rho_s \partial_\tau - c\mathcal{A}_\tau) \hat{\psi}_c - \mathcal{H}_m$ with the Hamilton $\mathcal{H}_m = \frac{\hbar^2}{2M_m} (-i\nabla - c\mathcal{A}_r - \mathcal{A}_T)^2 + \mathcal{F} \exp(-\frac{\Delta}{a}) \sin^2 \frac{x}{\Delta} + nmh_z + \frac{\epsilon_{dm}^2 a^2}{2\epsilon_{ne}} - c\epsilon_{ah} a^2 + \frac{n}{4\rho_n} + \epsilon_{an} a^2 (1 - 2 \operatorname{sech}^2 \frac{x}{\Delta})$, magnon mass $M_m = 4\hbar\rho_n/a^2$, and thermal vector potential $\mathcal{A}_T = \nabla T/T$. The magnon flow interacting with DWs in Eq. (1) is generated by thermal gradients, i.e. $j_m = \delta\mathcal{L}_m/\delta\mathcal{A}_T$. By the variational deductions $\hat{\mathcal{L}}_m/\hat{\psi}_c^\dagger$ and $\hat{\mathcal{L}}_m/\hat{\psi}_c$, we obtain the magnon-density ($\hat{\Xi}_c = \hat{\psi}_c^\dagger \hat{\psi}_c$) evolution equation

$$\partial_\tau \hat{\Xi}_c = \frac{i}{\hbar} [\hat{\Xi}_c, \mathcal{H}_m] + i(\rho_n \partial_\tau^2 - \alpha \partial_\tau) \hat{\Xi}_c + 2\frac{\tilde{\alpha}}{\hbar} (\hat{\Xi}_c U_w) \hat{\Xi}_c. \quad (3)$$

When magnons interplay with DWs in more comprehensive inelastic processes [159] [Fig. 7(b)], we divide the magnon field into the incident and scattered parts, i.e. $\hat{\psi}_c^\dagger = \frac{\tanh x - ik}{1 - ik} \exp[i(kx - \omega\tau)] + \frac{\tanh \ell + ik}{1 + ik} \frac{S(\phi)}{\sqrt{-i\ell}} \mathcal{I}(\phi) \exp[-i(k\ell - \omega\tau)]$ with the wavenumber k , frequency ω , elastic scattering amplitude $S(\phi)$, inelastic scattering trajectory $\mathcal{I}(\phi)$, and deflection path

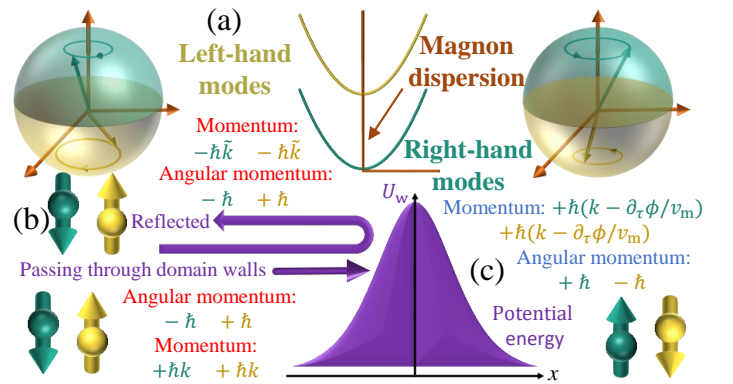


FIG. 6. (a) Ferrimagnetic magnons having left and right chiral modes. (b) Angular momentum of magnons reflected by DWs does not change, but their momentum varies $\hbar(\tilde{k} + k)$, and there is $\tilde{k} = k$ when scatterings are elastic. (c) Angular-momentum and momentum of magnons transmitting through DWs change $2\hbar$ (spin torque) and $2\hbar\partial_\tau\phi/v_m$ (redshifts), respectively, and it is accompanied by diabatic spin dislocations and redshifts when passing through DWs. Magnon energy of left and right polarization is different and is a function of ρ_s . When the spin density ρ_s is equal to 1, magnons are all right-handed (ferromagnetism); when it is equal to 0, magnon left and right polarization is degenerate (antiferromagnetism). Boson flows depend on choices of gauge potential [142], which is the physical mechanism by which we can regulate magnon scatterings via magnetic fields (\mathcal{A}_h), temperature (\mathcal{A}_T), and DWs (\mathcal{A}_μ).

$\ell = x \sec \phi$. Thus, we define the reflectance as $\mathcal{R} = \frac{1}{\Delta} \int_{-\frac{\pi}{2}}^{\frac{3\pi}{2}} S^\dagger(\phi) S(\phi) \operatorname{Re} \mathcal{I}(\phi) d\phi$ with the total cross-section $\Delta = \int_0^{2\pi} S^\dagger(\phi) S(\phi) \operatorname{Re} \mathcal{I}(\phi) d\phi = \frac{4}{k} \sum_{l=-\infty}^{+\infty} \sin^2 \vartheta_l$, Aharonov-Bohm phase shift ϑ_l [77, 78], and partial wave l .

$\mathcal{I}(\phi) = 1$ infers complete elastic scatterings, $\mathcal{I}(\phi) = 0$ means that magnons are absorbed by DWs, and $\mathcal{I}(\phi) > 1$ means that the number of reflected particles is increased by $\mathcal{I}(\phi) - 1$ times by releasing magnons from DWs. Subsequently, by the optical theorem [159], we extract the situation of complete transmission magnons

$$\operatorname{Im} S(0) \operatorname{Re} \mathcal{I}(0) = \sqrt{\frac{2}{k\pi}} \sum_{l=-\infty}^{+\infty} \sin^2 \vartheta_l = \sqrt{\frac{k}{8\pi}} \Delta, \quad (4)$$

evincing that the verdict of broad DWs and high-frequency magnons facilitating transmissions in the introductions is accurate.

Distinctively, when magnon energy approaches to DWs (DW quantized energy levels are given in Refs. [160, 161]), resonances will emerge, evoking scattering amplitudes to increase significantly. The energy eigenvalue is plurality popularized as $E_m = E_0 - \frac{1}{2}i\Gamma$, where the physical implication of Γ can be interpreted as the resonance width. Supplanting this complex energy into Eq. (3), the phase shift will have an excessive term $\delta\vartheta_l = -\operatorname{arc tan} \frac{\Gamma\vartheta_l}{2(E-E_0)}$ with a new resonance amplitude

$$S_\Gamma(\phi) = -\frac{\mathcal{I}\Gamma(2l+1)/2^l l! \sqrt{k} d^l (\cos^2 \phi - 1)^l}{[2(E_m - E_0) + i\Gamma]} e^{2i(\delta\vartheta_l)} \quad (5)$$

with $\Gamma = \frac{\hbar}{\alpha a} \left[\frac{\epsilon_{ne}}{n} k + \frac{\epsilon_{dm}(\omega - \epsilon_{dm}k/n)}{\epsilon_{an} + 2\epsilon_{ah} + 2\epsilon_{ne}k^2} \right]$. Compared with ferromagnetism, ferrimagnetism has additional nutation resonance modes [50], leading to stronger momentum transfers and weaker adiabatic spin torque.

After passing through (redshifts [133]) or being reflected by (scatterings [98, 162]) DWs, magnons momentum transfers will always occur [Fig. 7(b)]. We obtain the momentum-transfer intensity owing to scatterings by the variation $\beta_R = -\int \frac{\delta \mathcal{L}_w}{\hbar \delta(\partial_\tau \hat{\zeta}^\dagger)} \nabla \hat{\zeta}^\dagger \cdot dr \sim \Delta k$. For redshifts, their presence is because the wavenumber alters $2\partial_\tau \phi/v_m$ when magnons pass through DWs. Analogous to the magnon wavenumber variation $2k$ after being scattered, we define the redshift intensity as $\beta_r = \Delta \partial_\tau \phi/v_m$ [Fig. 7(c)]. Ultimately, the magnon adiabatic or diabatic torque intensity [94] is $\Omega_s = 1$ or $\beta_s = \alpha$.

Transition to observation representations. In actual observations, we should embody the above microcosmic imagery in measurable representations, of which one of the most straightforward is the DW velocity $\partial_\tau x = v$. From Eq. (1), we realize that the coefficient before the magnetic anisotropy ϵ_{an} is positive at a small DMI ϵ_{dm} , i.e. $\epsilon_{ne}\epsilon_{an} > |\epsilon_{dm}|$, constructing Néel-type DWs. For Néel DWs, Eq. (1) subsists a kink-soliton solution $n = (\operatorname{sech} \frac{x}{\Delta} \cos \zeta x, \operatorname{sech} \frac{x}{\Delta} \sin \zeta x, q \tanh \frac{x}{\Delta})$ with the topological charge $q = \frac{1}{\pi} \int_{-\infty}^{\infty} \nabla \theta dx = 1$, and the DW width is $\Delta = \sqrt{\epsilon_{ne}/\epsilon_{an}}$ in desirable-undisturbed status. At the new representation (x, ϕ) , through a variational operation $\frac{d}{dt} \frac{\delta \hat{\mathcal{L}}_w}{\delta(\partial_\tau \hat{\zeta}^\dagger)} - \frac{\delta}{\delta \hat{\zeta}^\dagger} (\hat{\mathcal{L}}_w + \hat{\mathcal{L}}_d) = -\frac{\delta \hat{\mathcal{L}}_d}{\delta(\rho_n \partial_\tau \hat{\zeta}^\dagger)}$ with $\partial_\tau \hat{\zeta}^\dagger = \partial_\tau \theta(x) \partial_{\theta(x)} \hat{\zeta}^\dagger + \partial_\tau \phi(x) \partial_{\phi(x)} \hat{\zeta}^\dagger$ ($\partial_\tau n = -v \nabla n + \hat{z} \times n \partial_\tau \phi$), we deduce the DW motion equations

$$\begin{aligned} & \frac{\rho_s + \alpha \zeta \Delta}{q + \zeta^2 \Delta^2} \Delta \partial_\tau \phi + \alpha \partial_\tau x + \rho_n \partial_\tau^2 x \\ &= -v_{px} \sin \frac{x}{\Delta} + \frac{m \Delta h_z}{(q + \zeta^2 \Delta^2)} + \bar{\beta} v_m \end{aligned}$$

and

$$\begin{aligned} & (\rho_s q - \alpha \zeta \Delta) \partial_\tau x - \alpha \Delta \partial_\tau \phi - \rho_n \Delta \partial_\tau^2 \phi = v_d \sin \phi - \\ & (v_a + v_{dip} + v_{p\phi}) \frac{q \pi \zeta \sin 2\phi}{\sinh(\pi \zeta \Delta)} - [(1 - \mathcal{R}) q \rho_s \Omega_s + \bar{\beta} \zeta \Delta] v_m \end{aligned} \quad (6)$$

with the reciprocal relation $[x, \phi] = \hbar a/2n$, $v_{px} \sim \epsilon_{px}$, $v_a \sim \epsilon_{ah}$, $v_{p\phi} \sim \epsilon_{p\phi}$, $v_{dip} \sim \epsilon_{dip}$, $v_d \sim \epsilon_{dm}$, and $\bar{\beta} = \mathcal{R} \beta_R - (1 - \mathcal{R})(\beta_s - \beta_r) - \beta_T$. At small external forces (below Walker-breakdown limits [163]), $\partial_\tau \phi = 0$ and $\phi = \pi$ hold true. On the premise of driving forces being weaker than pinning, DWs are crawling [164], and the solutions combined with Walker limits are (we write the solution of Eq. (6) as the form of Arrhenius's law [165, 166])

$$v = \bar{v}_p \sin(\omega_w \tau) + \left\{ \frac{m \Delta h_z}{\bar{\alpha}(q + \zeta^2 \Delta^2)} \exp\left(-\left|\frac{h_p}{h_z}\right|^{\chi_h}\right) + \right. \\ \left. \frac{\bar{\beta}_\phi}{\bar{\alpha}} v_m \exp\left(-\left|\frac{\nabla T_p}{\nabla T}\right|^{\chi_{\nabla T}}\right) \right\} (1 - e^{-\frac{\tau}{\bar{\tau}}}) \exp\left(-\left|\frac{T_p}{T}\right|^{\chi_T}\right) \quad (7)$$

with the pinning strength parameters h_p (χ_h), ∇T_p ($\chi_{\nabla T}$), and T_p (χ_T), relaxation time $\bar{\tau} \approx \bar{\alpha}/(\rho_n + \alpha)$, DW angular frequency (it is zero below Walker limits) $\omega_w = (v_0^2 - v_p^2)^{1/2} / [(\rho_s q - \alpha \zeta \Delta) \frac{(\rho_s + \alpha \zeta \Delta)}{\alpha(q + \zeta^2 \Delta^2)} + \alpha] \Delta$, $v_0 = [(1 - \mathcal{R}) q \rho_s \Omega_s + \bar{\beta} \zeta \Delta + \frac{\bar{\beta}}{\alpha} (\rho_s q - \alpha \zeta \Delta)] v_m + \frac{(\rho_s q - \alpha \zeta \Delta) m \Delta h_z}{\alpha(q + \zeta^2 \Delta^2)} - \frac{\rho_s q - \alpha \zeta \Delta}{\alpha} v_{px} \sin \frac{x_0}{\alpha}$, $v_p = \frac{v_d}{2 \cos \phi_0} - \frac{q \pi \zeta (v_a + v_{dip} + v_{p\phi})}{\sinh(\pi \zeta \Delta)}$, $\bar{\alpha} \bar{v}_p = \frac{\rho_s + \alpha \zeta \Delta}{q + \zeta^2 \Delta^2} \frac{v_d}{2 \cos \phi_0} - \frac{\rho_s + \alpha \zeta \Delta}{q + \zeta^2 \Delta^2} \left(\frac{v_a + v_{dip} + v_{p\phi}}{\alpha} \right) \frac{q \pi \zeta}{\sinh(\pi \zeta \Delta)} - \frac{\sin x_0 / \Delta}{v_{px} \sin 2\phi_0}$, $\bar{\alpha} = \alpha + \frac{\rho_s + \alpha \zeta \Delta}{q + \zeta^2 \Delta^2} \left(\frac{\rho_s q}{\alpha} - \zeta \Delta \right)$, $\bar{\beta}_\phi =$

$\bar{\beta} = \frac{\rho_s + \alpha \zeta \Delta}{(q + \zeta^2 \Delta^2) \alpha} [(1 - \mathcal{R}) q \rho_s \Omega_s + \bar{\beta} \zeta \Delta]$, and the solution of unknown quantities (x_0, ϕ_0) is in Supplementary Materials. h_p and ∇T_p are depinned by external driving forces [164], and T_p is depinned by thermal activation [167] that increases DW energy to make them surmount pinning cushion. Eq. (7) signifies that adiabatic spin torque only works above Walker-breakdown points, and DWs will be entirely depinned when $h_z \gg h_p$, $\nabla T \gg \nabla T_p$, or $T \gg T_p$.

Thermal spin-motive force. Moving DWs will spawn spin locomotion, making "Berry phases acting as magnetic vector potential" vary with time to energize voltages [28], which can also be regarded as inverse effects [168–170] of current-induced spin transfer torque and spin orbit torque [Fig. 7(a)]. Spontaneously, if we wield thermal gradients to compel DW motion, the concepts of thermoelectric generation [171] and electrical refrigeration [29] will be appeared. Hereby, the widely adopted thermoelectric figure of merit [172] expounding to spin-motive force can be comparably expounded as $\mathcal{E}_{TE} = S^2 T / \varrho \kappa$ with the resistance ϱ , Seebeck coefficient S , and heat conductivity κ . DW functions are to furnish spin voltages to intensify Seebeck coefficients and reduce thermal conductance by reflecting magnons [173] or consuming DW entropy [68]. Here we give the expression of its ferrimagnetic counterpart as

$$\begin{aligned} \mathcal{V}_w = \frac{\hbar}{e} p N \int [(\rho_s + \rho_{SOT} \sin \phi) - (\beta_{STT} + \beta_{SOT} \sin \phi) n \\ \times A_\mu] \cdot dr = -\frac{\hbar p N}{e \Delta} \{(\beta_{STT} + \beta_{SOT} \sin \phi + q \Delta \zeta) v \\ + [q - (\beta_{STT} + \beta_{SOT} \sin \phi) \Delta \zeta] \Delta \partial_\tau \phi\}, \end{aligned} \quad (8)$$

and the DW-devoted Seebeck coefficient can be portrayed as $S = -\frac{\mathcal{V}_w}{L \nabla T} = \frac{\hbar p N}{e \Delta L \nabla T} (\beta_{STT} + \beta_{SOT} \sin \phi) v$ with the system length L , diabatic spin-torque intension β_{STT} , effective spin-orbit-torque adiabatic or diabatic intension ρ_{SOT} or β_{SOT} [174], spin polarization p , DW number N , and charge e . The current corresponding to Eq. (7) is $j_e = \frac{e}{2\pi} \operatorname{Im} \operatorname{Tr} [\frac{\partial S_L}{\partial \tau} S_L^\dagger]$, and then we can define the resistance including DW contributions [175–178] as $\varrho_{STT} = \mathcal{V}_w/j_e$, while the Pt resistance ϱ_{SOT} is only born of electron-phonon scatterings. For another, as thermotransport mediums, magnons herein surpass phonons and electrons [173] (magnons will scatter electrons and phonons [179], making them inactive [180], especially for $k_B T \sim \epsilon_{an} a^2$), and this thermal conductivity can be expressed as $\kappa_m = \frac{\hbar}{4\pi T L} \operatorname{Tr} [\frac{\partial S_L}{\partial \tau} \frac{\partial S_L^\dagger}{\partial \tau}]$ by the scattering matrix of Eq. (5). For the non-magnetic metal layer Pt, the thermal conductivity κ_e is dominated by electrons evoked by the inverse spin-orbit torque. Perusing some pertinent calculations [29, 68, 137, 176–178], we garner the thermoelectric figure of merit with adopting $q = 1$ [Fig. 7(a)]

$$\mathcal{E}_{TE} = \frac{2\sqrt{k_B T + nmh_z}}{3n\Delta L \sqrt{\epsilon_{ne}} (\alpha\pi e)^2} \left\{ \left(\frac{\tilde{\beta}_{STT}}{\sqrt{\varrho_{STT}}} + \frac{\kappa_m}{\kappa_e} \frac{\beta_{SOT} \sin \phi}{\sqrt{\varrho_{SOT}}} \right) \right. \\ \left[(\bar{\beta} + \Delta \zeta) e^{-\left|\frac{\nabla T_p}{\nabla T}\right|^{\chi_{\nabla T}}} + \frac{m \Delta h_z}{v_m} e^{-\left|\frac{h_p}{h_z}\right|^{\chi_h}} \right] a \hbar p N e^{-\left|\frac{T_p}{T}\right|^{\chi_T}} \right\}^2 \quad (9)$$

with $\tilde{\beta}_{STT} = \beta_{STT} + \frac{q \rho_s}{\rho_s + \alpha} + \Delta \frac{\epsilon_{dm}}{\epsilon_{ne}} \frac{(q - \beta_{STT} - \beta_{SOT} \sin \phi) \rho_s + q \alpha}{\rho_s + \alpha}$. This thermoelectric figure of merit can also characterize the spin-Peltier refrigeration utility: moving DWs will dissipate energy by inelastic scatterings of releasing magnons, i.e. $\mathcal{E}_{Peltier} = \varrho \kappa T \mathcal{E}_{TE}$ [Fig. 7(b)]. By contrast, the thermoelectric figure of merit of ferromagnetic insulator DWs in Ref.

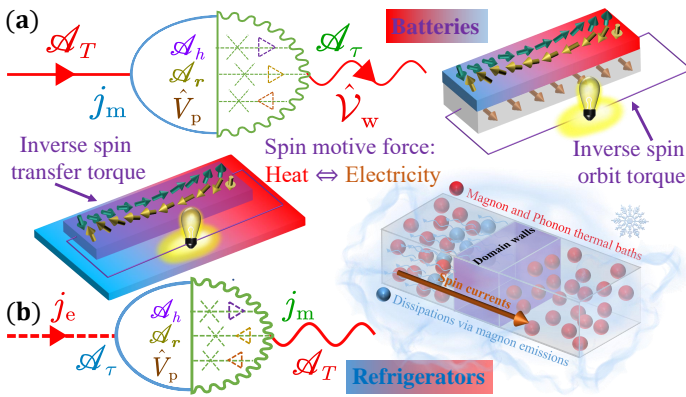


FIG. 7. (a) The thermal-gradient-excited magnon flow j_m interacts with the DW \mathcal{A}_r under the magnetic field \mathcal{A}_h and pinning impurity \hat{V}_p to convert the time-varying Berry phase \mathcal{A}_τ to the spin-motive force \hat{V}_w . (b) The inverse effect of thermal spin-motive force, i.e. current-driven DW motion for cooling, where energy is dissipated by releasing magnons through DWs subjected to particle-bath friction.

[29] is the magnetic Seebeck effect [181], i.e. the competence of thermal gradients to convert into magnon flows or effective magnetic fields.

DW dynamics under thermal gradients. Initially, we discuss the necessity of finite-temperature correction. Figs. 8(a)-(b) reveal that ferrimagnetism is more sensitive to temperature than ferromagnetism and antiferromagnetism. At the magnetization compensation temperature T_m , systems are immune to external magnetic fields ($m = 0$) but have limited spin angular momentum ($\rho_s \neq 0$). At the angular momentum compensation temperature T_s , angular momentum disappears ($\rho_s = 0$), but there is limited magnetization ($m \neq 0$). It is these individual features that allow ferrimagnetism to combine the advantages ($m \neq 0$ and $\rho_s = 0$) of ferromagnetism ($m \neq 0$ and $\rho_s \neq 0$) and antiferromagnetism ($m = 0$ and $\rho_s = 0$). To further illustrate effects of temperature on dynamics, we rewrite Eq. (1) to $\rho_s \partial_\tau \mathbf{n} = -\mathbf{n} \times \mathbf{h}_{\text{eff}} + \alpha \mathbf{n} \times \partial_\tau \mathbf{n} - \rho_n \mathbf{n} \times \partial_\tau^2 \mathbf{n} - \tilde{\alpha} (\mathbf{n} \cdot \mathbf{h}_{\text{eff}}) \mathbf{n}$ (\mathbf{h}_{eff} [s^{-1}] stands for system energy in a form of effective magnetic fields). Equivalently, we have $\rho_s \mathbf{n} \cdot \partial_\tau \mathbf{n} = \mathbf{n} \cdot \mathbf{n} \times (-\mathbf{h}_{\text{eff}} + \alpha \partial_\tau \mathbf{n} - \rho_n \partial_\tau^2 \mathbf{n}) - \tilde{\alpha} (\mathbf{n} \cdot \mathbf{h}_{\text{eff}}) \mathbf{n}^2 \Rightarrow \frac{\rho_s}{2} \partial_\tau \mathbf{n}^2 = -\tilde{\alpha} (\mathbf{n} \cdot \mathbf{h}_{\text{eff}}) \mathbf{n}^2 \Rightarrow |\mathbf{n}| \sim \exp(-\int \mathbf{n} \cdot \mathbf{h}_{\text{eff}}(T) \tilde{\alpha}(\rho_s, T) dT)$, certifying that the role of temperature enables the hitherto-widely-used zero-temperature spin-dynamics equation (i.e. $\tilde{\alpha} = 0$) to be defeated. Because the restriction $\partial_\tau \mathbf{n}^2 = 0$ in the zero-temperature equation ($\tilde{\alpha} = 0$) leads to spin-vector-length conservation, a misconception will emerge that magnetization still exists even at Néel or Curie temperature. Given this idea, there is no room for the consideration of the compensation points T_m and T_s . As a result, the previous studies [47, 63, 132] which adopted the zero-temperature equation to analyze ferrimagnetism will produce a widely differing consequence, with the infinite divergence of the gyromagnetic ratios and damping parameters. In fact, extending to finite temperature is a vital requirement [182] in examining DW-entropy influences because it essentially derives from the spin vector length reducing with temperature, i.e. $\partial_\tau |\mathbf{n}| = \partial_T |\mathbf{n}| \nabla T v$, and all interaction parameters are proportional to $(\partial_T |\mathbf{n}|)^\eta$ with the respective power relation η .

Then, we will demonstrate that magnon momentum transfers (cold) can be strong enough to exceed magnon spin-transfer torque (hot) and entropy forces (hot) and are

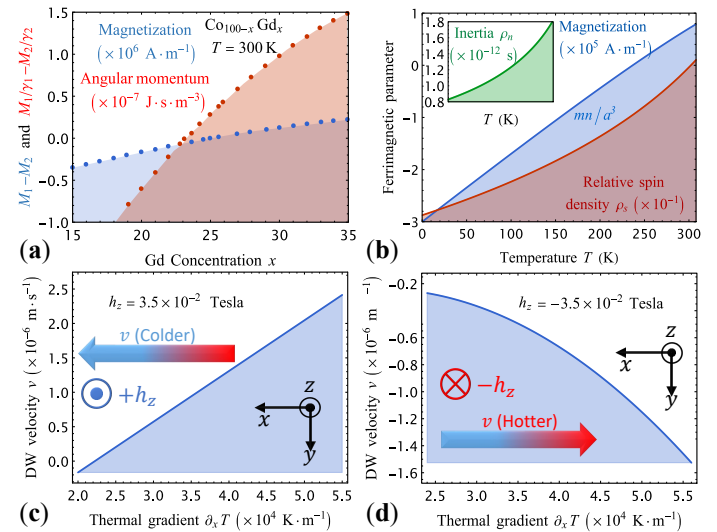


FIG. 8. Below Walker-breakdown limits + At crawling intervals. (a) Magnitudes of magnetization and angular-momentum vary with Gd contents at $T = 300\text{K}$ (experimental data selected from Ref. [183]). (b) Parameters characterizing ferrimagnetic natures vary with temperature at $\text{Co} : \text{Gd} = 80 : 20$. (c) DW velocities vary with thermal gradients. (d) DW velocities vary with thermal gradients when magnetic fields in (c) are reversed.

thereby capable of propelling DWs to cold regions. Firstly, we add a magnetic field in the $+z$ direction to make DWs move towards cold regions and detect that DW velocities increase with thermal gradients [Fig. 8(c)]. Nevertheless, this increasing trend can not be solely explained as the role of momentum because magnetic-field-driven DW motion with thermal activation [Eq. (7)] can also evoke the similar result [27]. We thereafter flip magnetic fields and find that, while velocities still increase with thermal gradients [Fig. 8(d)], they do so to a smaller extent than that depicted in Fig. 8(c). This unfolds that the contribution of magnetic fields to velocities is larger than that of thermal gradients so that velocity magnitudes keep increasing with thermal gradients due to depinning by thermal activation. Basically, magnon momentum transfers can be embodied in the following two facets: (1) the existence of magnon momentum transfers engenders velocities in Fig. 10(a) greater than that in Fig. 10(b); (2) the nonlinearity of velocities and thermal gradients in Fig. 8(d) is stronger than that in Fig. 8(c), indicating that DWs in Fig. 8(d) suffer lesser forces due to their motion directions opposite to that contributed by magnons. Consequently, magnon momentum-transfer proportions are the difference between velocities in Figs. 8(c)-(d) or Figs. 10(a)-(b). Ref. [184] supports our conclusion via atomic-spin-dynamics simulations, i.e. finding that small radius skyrmions will move to cold regions at low damping. This is a result of momentum transfers because scatterings will stand above thermal diffusion under low damping and small radii.

Identically, DW motion towards cold ends reported in Ref. [58] is also the combined effect of magnetic fields and momentum transfers rather than the Nernst-Ettingshausen mechanism. From this viewpoint, Ref. [57] can not well prove the existence of magnon momentum transfers because it does not exclude influences of magnetic fields. Actually, the phenomenon [101] that skyrmions rotate around the disk center can not also justify the existence of momentum transfers because the entropy force F and magnon scatterings can cause the same velocity in the y -direction,

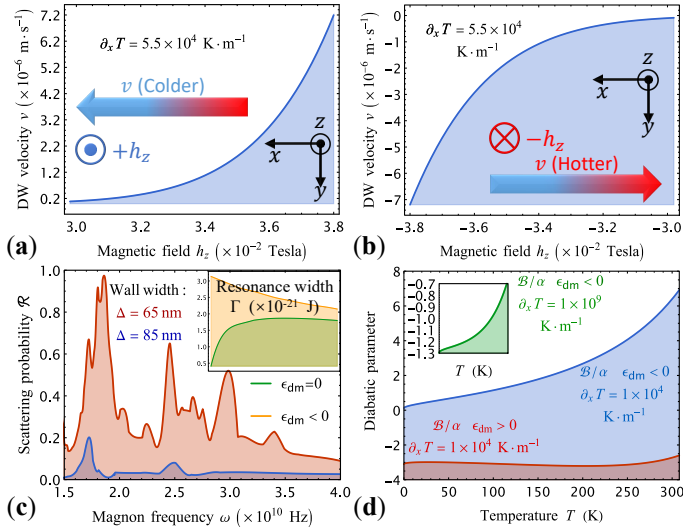


FIG. 9. (a)-(b) DW velocities vary with magnetic fields below Walker-breakdown limits (in crawling intervals). (c) Influences of magnon frequencies and DW widths on scatterings. (d) The total diabatic parameter β_ϕ/α including magnon momentum, magnon angular momentum, entropy effects, and DMIs varies with temperature under different thermal gradients (below Walker-breakdown limits). Positive or negative values of this parameter represent DW motion towards cold or hot regions, respectively.

i.e. $v_y^{\text{sky}} = \frac{4\pi q(4\pi\alpha v_m + F)}{(\alpha \int \partial_x \mathbf{n} \cdot \partial_y \mathbf{n} dx dy)^2 + 16\pi^2 q^2}$. In particular, the phenomenon [26] of skyrmion migration to cold ends is because a large number of skyrmions produced in high-temperature regions will repel each other, and this repulsive force can push skyrmions to cold regions (relevant simulation and numerical-comparison results are shown in Refs. [135, 185]). A recent experiment [56] subsequently reports that skyrmion motion directions will be reversed from cold to hot regions when thermal gradients continue to increase, consistent with the conclusion of Refs. [135, 137] (since many factors are not considered, Ref. [186] only draws a conclusion that DW velocities increase with temperature under a fixed thermal gradient). When $\Delta k = 1$, momentum transfers and resonances enhanced by DMIs are strongest due to the scattering intensity $\beta_R \sim \Delta k$ and scattering rate $\mathcal{R} \sim 1/\Delta k$ [Fig. 10(c)], resembling to the cases [91, 117] of magnons scattered by skyrmions. Scattering intensity of DWs to left and right chiral magnons is different [187], and the relative number of two chiral magnons is affected by the spin density ρ_s , but its influence is not as great as the above factors. Large thermal gradients will enhance magnon frequencies and excite soliton inner modes (i.e. $\partial_\tau \phi \neq 0$), facilitating spin torque to move towards hot regions [Fig. 10(d)].

We go on to show that the principal cause of DW migration to hot regions is not magnon spin torque but DMI vector potential and entropy forces. When thermal gradients are so massive that DWs are above Walker-breakdown limits ($\partial_\tau \phi \neq 0$), adiabatic spin torque and redshifts will work [Eq. (7)]. Whereas large thermal gradients are likely to accompany by global high temperature, this will simultaneously increase magnon wavenumbers and DW widths, reducing scattering rates [Eq. (4) and Fig. 10(c)]. Because redshifts-induced momentum transfers are proportional to DW angular frequencies, their effects are to increase velocities by a factor of $\frac{(1-\mathcal{R})\rho_s}{(\rho_s-1+\mathcal{R})\rho_s+\alpha^2}$ but not to impact on velocity directions, i.e., we can eliminate $\beta_r \sim \partial_\tau \phi$ when we solve Eq. (6) [see Eq. (7)]. Another effect of the Walker-breakdown

occurrence is that it can enhance the easy-axis anisotropy $\epsilon_{an} + \rho_n n (\mathbf{n} \times \mathbf{e}_z \partial_\tau \phi/a)^2$ to increase magnon reflectivity, but its comprehensive influence will still push DWs toward hot regions when ρ_s is considerable [Fig. 10(d)].

However, if we reverse the DMI sign, DW motion directions can be reversed [Fig. 10(d)]. DMIs resemble dipole fields [188], inducing hard-axis anisotropy and jointly twisting the

DW width as [189] $\Delta^2 = \frac{4\epsilon_{ne}(4\epsilon_{an}-\epsilon_{dm}^2/\epsilon_{ne})^{-1}}{1+\epsilon_{ah}\sin^2\phi/[\epsilon_{an}-\nu(M_1-M_2)^2/2]}$. Generally, DMIs have the following functions: (1) decreasing magnon reflectivity by increasing DW widths and causing additional scattering potential [Eqs. (3)-(4)]; (2) devoting an extra entropy force that always makes DWs trend towards cold regions because $\pi\epsilon_{dm}\cos\phi > 0$ in Eq. (2) ($\epsilon_{dm} > 0 \Rightarrow \phi = 0$ and $\epsilon_{dm} < 0 \Rightarrow \phi = \pi$) (but here it doesn't exceed effects of Heisenberg and anisotropic interactions, see Fig. 5); (3) attracting additional DMI magnon flows to make DWs move towards hot ($\frac{(1-\mathcal{R})q\rho_s\Omega_s+\beta\zeta\Delta}{\alpha\zeta\Delta-\rho_sq-\alpha^2\frac{q+\zeta^2\Delta^2}{\rho_s+\alpha\zeta\Delta}} < 0$) or cold ($\frac{(1-\mathcal{R})q\rho_s\Omega_s+\beta\zeta\Delta}{\alpha\zeta\Delta-\rho_sq-\alpha^2\frac{q+\zeta^2\Delta^2}{\rho_s+\alpha\zeta\Delta}} > 0$) regions [$v \sim \frac{(1-\mathcal{R})q\rho_s\Omega_s+\beta\zeta\Delta}{\alpha\zeta\Delta-\rho_sq-\alpha^2\frac{q+\zeta^2\Delta^2}{\rho_s+\alpha\zeta\Delta}} v_m$ in Eqs. (6)-(7)]; (4) enhancing [190] amplitudes by a negative sign or attenuating [190] amplitudes by a positive sign [the resonance width in Eq. (5)]; (5) intensifying ferrimagnetic properties of translation and rotation freedom-degree couplings and making relaxation time not always positive [Eqs. (6)-(7)] (especially when DMIs are relatively large, DWs can be accelerated throughout the whole movement process). In these competitive relationships here, the third effect is dominant: contributions of magnons to DW velocity directions are inverse when DMI signs are reversed [Fig. 10(d)]. Ferromagnetic micromagnetic-simulations [61, 88] and ferromagnetic and antiferromagnetic micromagnetic-calculations [191] bear out our contention, and the experiment [192] also observe that a positive DMI sign will make DWs move towards magnon sources (hot ends).

The observed tendency [52] of DW motion to hot regions is therefore due to influences of vector potential caused by DMIs on magnon scatterings. Differently, the reference [55] supposes that magnon spin torque pull DWs towards hot regions because DWs still move when thermal gradients are gradually reduced to zero. While thermal gradients are zero, magnon flows will not disappear immediately due to finite diffusion lengths so they can continue to drive DWs. Nevertheless, in the absence of magnons, only DW inertia can also make DWs slide for certain distances so the above phenomenon [55] should be interpreted as the coalescent consequence of magnons and entropy forces. One of the pivotal factors is that spin torque is smaller than entropy forces, and its magnitudes caused by exchange interactions alone can be larger than magnon torque [60, 61]. In the experiment [53], there are no DMIs but hard-axis anisotropy stabilizing Bloch DWs. Analogously, this does not prove that magnon spin torque make DWs move towards hot regions because more significant entropy forces are not excluded. Summing up, phenomena of DWs moving towards hot regions observed by them are actually caused by entropy forces because magnon amplitudes and their reflection on DWs are reduced when DMI signs are reversed or DMIs are equal to zero ($- \rightarrow +/0$).

Eventually, the investigation [63] of ferrimagnetic DW dynamics under thermal gradients cannot explain our experimental phenomena, for reasons which we have explained in our introductions. Distinctively, by micromagnetic simu-

lation, Ref. [193] finds skyrmions moving to cold ends with spiral backgrounds [194] induced by large DMIs, because these backgrounds will provide boundary forces conducive to motion towards cold regions. The article [16] indicates that a structure called skyrmion-DWs can have Rosen-Morse potential with total reflection, and DWs and easily-excited gapless magnons formed in systems with second-order magnetic anisotropy also have ascendant reflectivity [110]. As we mentioned earlier, DW-structure changes and variations of various interactions are the same, which all modify system Lagrangian and thus affect magnon reflectivity. If DMI strength becomes large enough, DWs will have additional rotational degrees of freedom [195], but our conclusion is still valid because this can be eliminated by ϕ , equivalent to multiplying DW velocities by a coefficient.

Power generation and refrigeration by heat-spin reciprocities. Spin motive force depends on DW velocities under thermal gradients [Eq. (7)], which embodies change speeds of Berry phases, and having tremendous impacts on the changing rates is pinning [Figs. 11(a)-(b)]. Among them, interference of magnetic impurities on DW motion is weaker than that of elastic impurities because only adiabatic spin torque can immediately contribute to velocities through ϕ [Fig. 11(a)]. Moreover, DWs propelled by thermal gradients have a merit in depinning, i.e., they can preferably surmount impurities due to thermal activation [Figs. 8(c)-(d)] (antiferromagnetic couplings will strengthen this effect [196], compared with ferromagnetic DWs [197]). Another quantity having conspicuous influences on velocities is the relative spin density ρ_s , and velocities will accomplish the maximum at $\rho_s = 0$ [Figs. 11(b)-(c)], i.e., systems are completely anti-ferromagnetic couplings. Nonetheless, once systems are in these states, DWs will not oscillate and cannot output alternating voltages. This requires us to sacrifice some efficiency to swap a frequency ω_w controlled by thermal gradients, magnetic fields, and temperature [Eqs. (7)-(7), and Fig. 11(c)].

In the previous ferromagnetic vortex experiment [198], magnitudes ($\sim \mu\text{V}$) and frequencies ($\sim \text{ns}$) of spin-motive force are all considerable, and these will be further consolidated in ferrimagnetism. In any event, commercial levels ($\mathcal{E}_{\text{TE}} \geq 3$) can be fulfilled [Fig. 11(d)] if we can manufacture devices with smoother surfaces [150] and thinner films [153] to achieve tiny external and internal pinning (thinner thicknesses and smaller lengths-widths can reduce internal pinning caused by dipole fields and numbers of foreign impurities, respectively). Considering the DW count N and pinning proportional to the cross-sectional area A , we find $\mathcal{E}_{\text{TE}} \sim N^2/\Delta V$ with the device volume V . In small or large volume, there is $V \ll 1$ or $N \gg 1$, enunciating that spin motive force can demonstrate superior performances at any size.

Fig. 11(d) proclaims that magnetic fields and temperature can raise thermoelectric figures of merit, which they do by affecting magnons and DWs. As heat transport mediums [173, 199–201], low-energy magnons will be completely reflected. At significant thermal gradients, high-energy magnons with small DMIs are transmissive but will lose their energy when passing through precession DWs due to redshifts. We can also adjust DMI intensities so that magnons of various wavelengths are reflected [121]. Hence, the existence of DWs will invariably reduce thermal conductance and improve electrical conductance, breaking the confinement of the Wiedemann-Franz law like Ref. [202]. Magnetic

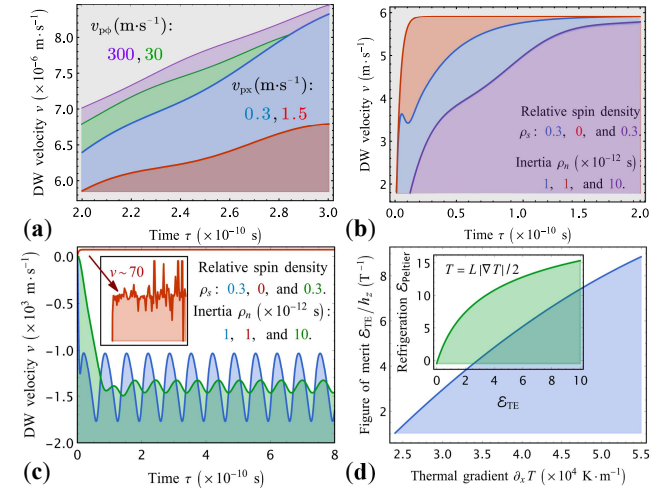


FIG. 10. (a) Influences of pinning strength on DW velocities below Walker-breakdown limits (in crawling intervals). (b)-(c) Influences of ferrimagnetic characteristic parameters on DW velocities below(b) or above(c) Walker-breakdown limits (in depinning intervals). (d) The influences of magnetic fields and temperature on thermoelectric figures of merit.

fields and temperature can regulate magnon energy and can be usefully employed to depin DWs to ulteriorly enhance thermoelectric figures of merit [Eq. (8)]. Even if there are phenomenal thermal gradients (high energy magnons), we can still wield bigger magnetic fields [125, 200, 203], DMIs [121, 203], and DW structure potential [16] to make magnons be completely reflected. Furthermore, magnons can also form non-dissipative and non-thermal-conductive superfluids [204] in a wide range of temperature and magnetic fields to increase electrical conductance and reduce thermal conductance concurrently and scatter with electrons to shape drag effects [179, 205–207] for amplifying the diabatic factor β_{STT} .

Spincaloritronics devices overcome the difficulty of thermoelectric-conversion disappearances due to electron-hole compensation, avert the constraint of the Wiedemann-Franz law constraining concurrent optimization of electrical and thermal conductance, and refine complex material stacks [208]. Analogously, magnetic topological semimetals [5] and topological insulators [209–214] can also retain these excellences and fulfil better thermoelectric figures of merit. Magnetic semimetals have strong Berry curvature, while topological insulators have topological embodiment in reciprocal space (associated with real space of DWs). By contrast, DWs have advantages in miniaturization, low-energy consumption, and high-temperature resistance. All these features are ascribed to huge emergence of spin Berry phases [4, 215, 216] [Fig. 12], and generated electrons with spin degrees of freedom have greater chemical potential [217] to enhance charge accumulations.

The inverse effect of spin thermoelectricity, i.e. cooling, it stems from the fact that DWs subjected to frictional forces will dissipate energy by emitting magnons. Different from the spin Peltier effect [207, 218] of only exchanging energy of magnons and phonons, the existence of DWs makes magnons affected by Berry phases generate non-Markovian friction so that environments and systems are more closely related.

In practical applications, mutually perpendicular temperature gradients and voltage directions can better achieve separations of electrons and heat flows to break the Wiedemann-

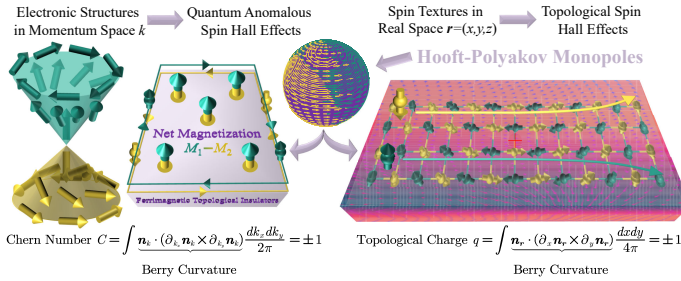


FIG. 11. Different manifestations of non-Abelian Berry phases generated by Hooft-Polyakov magnetic monopoles in momentum and real space.

Franz law. We can replace DWs with vortex walls [219] or skyrmions [220] to implement this transverse thermoelectric effect, i.e., the relationship between the direction of voltages and velocities is $\mathcal{V}_w e_y \sim v e_x$ in Eq. (7).

No experiments characterize influences of various factors on thermoelectric figures of merit in detail but only estimate the order of magnitudes in Fig. 10(d) based on existing measurement results. For this realm, we still need to investigate effects of DWs with different widths, magnons with different frequencies, and static and alternating magnetic fields in any direction on thermal and electrical conductance.

Conclusions. We probe DW dynamics under thermal gradients in ferrimagnetism generalized to ferromagnetism and antiferromagnetism and analyze magnon momentum transfers, shedding light on why DWs can move to hot (magnon spin torque and entropy forces) or cold (magnon momentum transfers) regions in experiments. We show that magnon momentum transfers are efficient driving forces and is much stronger than spin torque. We uncover that time-varying spin Berry phases induced by thermal gradients can elicit a commercial-level thermoelectric figure of merit that will maintain advantages in diminutive-volume elements and at high temperature. We hope that different forms of Berry phases can be more widely used in practical applications [221], such as topological insulators, topological semi-metals, axion insulators, topological superconductors, and topological solitons [Fig. 12]. Our work indicates ways forward for green spincalortronics and topological quantum materials in the post-Moore era.

Appendix

Using path integrals directly will cause integrand functions having classical-action forms, contrary to quantum essence of spins. In spin motion equations, generalized velocities rather than acceleration are proportional to generalized forces, and generalized forces are perpendicular to velocity directions. The above consideration shows that Hamilton's principle cannot describe spin motion, and we resort to coherent state formalism here to obtain complete spin action and paths. We write the spin coherent state $|s\rangle$ as

$$|s\rangle = |\hat{s}\rangle = \begin{pmatrix} e^{-i\phi} \cos \frac{\theta}{2} \\ \sin \frac{\theta}{2} \end{pmatrix} \text{ with } \int \frac{1}{2\pi} |s\rangle \langle s| d^2s = \begin{pmatrix} 1 & 0 \\ 0 & 1 \end{pmatrix}. \quad (10)$$

Inserting $\int |s\rangle \langle s| \frac{d^2s}{2\pi}$ into $\langle s_j | s_k \rangle$, we can obtain the complete path integral

$$\langle s_j | s_k \rangle = \int \prod_{i=1}^{\infty} \langle s(\tau) | s(\tau_i) \rangle \cdots \langle s(\tau_2) | s(\tau_1) \rangle$$

$$\times \langle s(\tau_1) | s(0) \rangle \frac{d^2s(\tau_1)}{2\pi}. \quad (11)$$

Because of

$$\begin{aligned} \langle s(\delta\tau) | s(0) \rangle &= \hat{\zeta}^\dagger \hat{\zeta} - \hat{\zeta}^\dagger(\delta\tau) [\hat{\zeta}(\delta\tau) - \hat{\zeta}(0)] \\ &= 1 - \hat{\zeta}^\dagger(\delta\tau) \frac{\partial \hat{\zeta}(\delta\tau)}{\partial \tau} \delta\tau \approx \exp \left(-\hat{\zeta}^\dagger \frac{\partial \hat{\zeta}}{\partial \tau} \delta\tau \right), \end{aligned} \quad (12)$$

we can rewrite Eq. (11) as

$$\begin{aligned} \langle s_j(\tau) | s_k(\tau) \rangle &= \int \exp(iS) \mathcal{D}^2 \left(\frac{s(\tau)}{2\pi} \right) \\ &\Rightarrow S = i \int_0^\tau \hat{\zeta}^\dagger \frac{\partial \hat{\zeta}}{\partial \tau} d\tau \end{aligned} \quad (13)$$

with the spin action S and measure \mathcal{D} of the space s , and Eq. (13) represents ferromagnetic Abelian phases. For ferromagnetism, we expand the spin s_i of each lattice point to the sum of Néel vectors and net spin vectors: $s_j = (-1)^j n + s$. Thus, the above Abelian Berry phases become non-Abelian, inducing the following motion equation:

$$2\delta S(\hat{\zeta}) / \delta \hat{\zeta} = \mathbf{n} \cdot (\partial_\tau \mathbf{n} \times \mathbf{s}) + \mathbf{n} \cdot (\partial_\tau \mathbf{n} \times \partial_r \mathbf{n}). \quad (14)$$

Using the transformation relation [222] between n and s to eliminate s and then expressing n by spinors, we can obtain the Berry phase of Eq. (1). The first and second terms in Eq. (14) are dynamic and topological terms, respectively. This topological term $S_{\text{top}} = \frac{1}{4\pi} \int \mathbf{n} \cdot (\partial_\tau \mathbf{n} \times \partial_r \mathbf{n}) dr d\tau$ has some similar effects with DMIs and is also the common origin of the topological spin Hall effect [223] and topological magneto-optical effect [224]. By variational operations for non-Abelian phases and considering [225] spin-flip and spin-phonon scatterings, we obtain the ferrimagnetic Landau-Lifshitz-Bloch equation $\rho_s \partial_\tau \mathbf{n} + \rho_n \mathbf{n} \times \partial_\tau^2 \mathbf{n} = -\mathbf{n} \times \mathbf{h}_{\text{eff}} + \alpha_{\text{eff}} \times \partial_\tau \mathbf{n} - \tilde{\alpha}(\mathbf{n} \cdot \mathbf{h}_{\text{eff}}) \mathbf{n}$, where non-Abelian Berry phases generate spin nutation and precession, while spin scatterings induce transverse and longitudinal damping. We also derive this equation from the usual spin-up and spin-down double-lattice-coupling method in [Supplementary materials](#).

Supplementary materials

A more detailed derivation of Eqs. (1) and (7) can be found in the supplementary information.

-
- [1] S. S. P. Parkin, M. Hayashi, and L. Thomas, Magnetic Domain-Wall Racetrack Memory, *Science* **320**, 190 (2008).
 - [2] Z. Luo, A. Hrabec, T. P. Dao, G. Sala, S. Finizio, J. Feng, S. Mayr, J. Raabe, P. Gambardella, and L. J. Heyderman, Current-Driven Magnetic Domain-Wall Logic, *Nature* **579**, 214 (2020).
 - [3] T. Yokouchi, F. Kagawa, M. Hirschberger, Y. Otani, N. Nagaosa, and Y. Tokura, Emergent Electromagnetic Induction in a Helical-Spin Magnet, *Nature* **586**, 232 (2020).
 - [4] A. Kitaori, N. Kanazawa, T. Yokouchi, F. Kagawa, N. Nagaosa, and Y. Tokura, Emergent Electromagnetic Induction beyond Room Temperature, *Proc. Natl. Acad. Sci. U.S.A.* **118**, e2105422118 (2021).
 - [5] J. Xiang, S. Hu, M. Lyu, W. Zhu, C. Ma, Z. Chen, F. Steglich, G. Chen, P. Sun, J. Xiang, S. Hu, M. Lyu, W. Zhu, C. Ma, Z. Chen, F. Steglich, G. Chen, and P. Sun, Large Transverse Thermoelectric Figure of Merit in a Topological Dirac

- Semimetal, *Sci. China-Phys. Mech. Astron.* **63**, 237011 (2020).
- [6] S. Roychowdhury, A. M. Ochs, S. N. Guin, K. Samanta, J. Noky, C. Shekhar, M. G. Vergniory, J. E. Goldberger, and C. Felser, Large Room Temperature Anomalous Transverse Thermoelectric Effect in Kagome Antiferromagnet YMn₆Sn₆, *Adv. Mater.*, **2201350** (2022).
- [7] Y. You, H. Lam, C. Wan, C. Wan, W. Zhu, L. Han, H. Bai, Y. Zhou, L. Qiao, T. Chen, F. Pan, J. Liu, and C. Song, Anomalous Nernst Effect in an Antiperovskite Antiferromagnet, *Phys. Rev. Applied* **18**, 024007 (2022).
- [8] J. Xu, J. He, J.-S. Zhou, D. Qu, S.-Y. Huang, and C. L. Chien, Observation of Vector Spin Seebeck Effect in a Noncollinear Antiferromagnet, *Phys. Rev. Lett.* **129**, 117202 (2022).
- [9] W. Lin, J. He, B. Ma, M. Matzelle, J. Xu, J. Freeland, Y. Choi, D. Haskel, B. Barbiellini, A. Bansil, G. A. Fiete, J. Zhou, and C. L. Chien, Evidence for Spin Swapping in an Antiferromagnet, *Nat. Phys.* **18**, 800 (2022).
- [10] T. Chen, T. Tomita, S. Minami, M. Fu, T. Koretsune, M. Kitatani, I. Muhammad, D. Nishio-Hamane, R. Ishii, F. Ishii, R. Arita, and S. Nakatsuji, Anomalous Transport Due to Weyl Fermions in the Chiral Antiferromagnets Mn₃X, X = Sn, Ge, *Nat. Commun.* **12**, 572 (2021).
- [11] M. Ikhlas, T. Tomita, T. Koretsune, M.-T. Suzuki, D. Nishio-Hamane, R. Arita, Y. Otani, and S. Nakatsuji, Large Anomalous Nernst Effect at Room Temperature in a Chiral Antiferromagnet, *Nat. Phys.* **13**, 1085 (2017).
- [12] K.-i. Uchida, W. Zhou, and Y. Sakuraba, Transverse Thermoelectric Generation Using Magnetic Materials, *Appl. Phys. Lett.* **118**, 140504 (2021).
- [13] K. Kuroyama, S. Matsuo, J. Muramoto, S. Yabunaka, S. R. Valentin, A. Ludwig, A. D. Wieck, Y. Tokura, and S. Tarucha, Real-Time Observation of Charge-Spin Cooperative Dynamics Driven by a Nonequilibrium Phonon Environment, *Phys. Rev. Lett.* **129**, 6 (2022).
- [14] P. Krystczko, X. Hu, N. Liebing, S. Sievers, and H. W. Schumacher, Domain Wall Magneto-Seebeck Effect, *Phys. Rev. B* **92**, 140405 (2015).
- [15] A. C. Niemann, T. Böhnert, A.-K. Michel, S. Bäßler, B. Gotsmann, K. Neuróhr, B. Tóth, L. Péter, I. Bakonyi, V. Vega, V. M. Prida, J. Gooth, and K. Nielsch, Thermoelectric Power Factor Enhancement by Spin-Polarized Currents-A Nanowire Case Study, *Adv. Electron. Mater.* **2**, 1600058 (2016).
- [16] S. Lee, K. Nakata, O. Tchernyshyov, and S. K. Kim, Magnon Dynamics in a Skyrmion-textured Domain Wall of Antiferromagnets, *arXiv:2211.00030* (2022).
- [17] B. Keimer and J. E. Moore, The Physics of Quantum Materials, *Nat. Phys.* **13**, 1045 (2017).
- [18] Y. Tokura, Quantum Materials at the Crossroads of Strong Correlation and Topology, *Nat. Mater.* **21**, 971 (2022).
- [19] K. Uchida, S. Takahashi, K. Harii, J. Ieda, W. Koshiba, K. Ando, S. Maekawa, and E. Saitoh, Observation of the Spin Seebeck Effect, *Nature* **455**, 778 (2008).
- [20] R. Cheng, S. Okamoto, and D. Xiao, Spin Nernst Effect of Magnons in Collinear Antiferromagnets, *Phys. Rev. Lett.* **117**, 217202 (2016).
- [21] E. Raimondo, E. Saugar, J. Barker, D. Rodrigues, A. Giordano, M. Carpentieri, W. Jiang, O. Chubykalo-Fesenko, R. Tomasello, and G. Finocchio, Temperature-Gradient-Driven Magnetic Skyrmion Motion, *Phys. Rev. Applied* **18**, 024062 (2022).
- [22] J. C. Slonczewski, Initiation of Spin-Transfer Torque by Thermal Transport from Magnons, *Phys. Rev. B* **82**, 054403 (2010).
- [23] M. Matsuo, Y. Ohnuma, T. Kato, and S. Maekawa, Spin Current Noise of the Spin Seebeck Effect and Spin Pumping, *Phys. Rev. Lett.* **120**, 037201 (2018).
- [24] G.-M. Choi, C.-H. Moon, B.-C. Min, K.-J. Lee, and D. G. Cahill, Thermal Spin-Transfer Torque Driven by the Spin-Dependent Seebeck Effect in Metallic Spin-Valves, *Nat. Phys.* **11**, 576 (2015).
- [25] G. E. W. Bauer, E. Saitoh, and B. J. van Wees, Spin Caloritronics, *Nat. Mater.* **11**, 391 (2012).
- [26] Z. Wang, M. Guo, H.-A. Zhou, L. Zhao, T. Xu, R. Tomasello, H. Bai, Y. Dong, S.-G. Je, W. Chao, H.-S. Han, S. Lee, K.-S. Lee, Y. Yao, W. Han, C. Song, H. Wu, M. Carpentieri, G. Finocchio, M.-Y. Im, S.-Z. Lin, and W. Jiang, Thermal Generation, Manipulation and Thermoelectric Detection of Skyrmions, *Nat. Electron.* **3**, 672 (2020).
- [27] J. Mazo-Zuluaga, E. A. Velásquez, D. Altbir, and J. Mejía-López, Controlling Domain Wall Nucleation and Propagation with Temperature Gradients, *Appl. Phys. Lett.* **109**, 122408 (2016).
- [28] S. A. Yang, G. S. D. Beach, C. Knutson, D. Xiao, Q. Niu, M. Tsoi, and J. L. Erskine, Universal Electromotive Force Induced by Domain Wall Motion, *Phys. Rev. Lett.* **102**, 067201 (2009).
- [29] A. A. Kovalev and Y. Tserkovnyak, Thermomagnetic Spin Transfer and Peltier Effects in Insulating Magnets, *Europhys. Lett.* **97**, 67002 (2012).
- [30] A. A. Kovalev and Y. Tserkovnyak, Magnetocaloritronic Nanomachines, *Solid State Commun.* **150**, 500 (2010).
- [31] A. A. Kovalev and Y. Tserkovnyak, Thermoelectric Spin Transfer in Textured Magnets, *Phys. Rev. B* **80**, 100408 (2009).
- [32] L. Shen, J. Xia, M. Ezawa, O. A. Tretiakov, G. Zhao, and Y. Zhou, Signal Detection Based on the Chaotic Motion of an Antiferromagnetic Domain Wall, *Appl. Phys. Lett.* **118**, 012402 (2021).
- [33] J. Zážvorka, F. Jakobs, D. Heinze, N. Keil, S. Kromin, S. Jaiswal, K. Litzius, G. Jakob, P. Virnau, D. Pinna, K. Everschor-Sitte, L. Rózsa, A. Donges, U. Nowak, and M. Kläui, Thermal Skyrmion Diffusion Used in a Reshuffler Device, *Nat. Nanotechnol.* **14**, 658 (2019).
- [34] A. Fernández Scarioni, C. Barton, H. Corte-León, S. Sievers, X. Hu, F. Ajedas, W. Legrand, N. Reyren, V. Cros, O. Kazakova, and H. W. Schumacher, Thermoelectric Signature of Individual Skyrmions, *Phys. Rev. Lett.* **126**, 077202 (2021).
- [35] J. M. Bartell, D. H. Ngai, Z. Leng, and G. D. Fuchs, Towards a Table-Top Microscope for Nanoscale Magnetic Imaging Using Picosecond Thermal Gradients, *Nat. Commun.* **6**, 8460 (2015).
- [36] H. Katsura, N. Nagaosa, and P. A. Lee, Theory of the Thermal Hall Effect in Quantum Magnets, *Phys. Rev. Lett.* **104**, 066403 (2010).
- [37] A. L. Chernyshev, Strong Quantum Effects in an Almost Classical Antiferromagnet on a Kagome Lattice, *Phys. Rev. B* **92**, 094409 (2015).
- [38] J. Yu, D. Bang, R. Mishra, R. Ramaswamy, J. H. Oh, H.-J. Park, Y. Jeong, P. Van Thach, D.-K. Lee, G. Go, S.-W. Lee, Y. Wang, S. Shi, X. Qiu, H. Awano, K.-J. Lee, and H. Yang, Long Spin Coherence Length and Bulk-like Spin–Orbit Torque in Ferromagnetic Multilayers, *Nat. Mater.* **18**, 29 (2019).
- [39] D.-H. Kim, T. Okuno, S. K. Kim, S.-H. Oh, T. Nishimura, Y. Hirata, Y. Futakawa, H. Yoshikawa, A. Tsukamoto, Y. Tserkovnyak, Y. Shiota, T. Moriyama, K.-J. Kim, K.-J. Lee, and T. Ono, Low Magnetic Damping of Ferrimagnetic GdFeCo Alloys, *Phys. Rev. Lett.* **122**, 127203 (2019).
- [40] T. Okuno, D.-H. Kim, S.-H. Oh, S. K. Kim, Y. Hirata, T. Nishimura, W. S. Ham, Y. Futakawa, H. Yoshikawa, A. Tsukamoto, Y. Tserkovnyak, Y. Shiota, T. Moriyama, K.-J. Kim, K.-J. Lee, and T. Ono, Spin-Transfer Torques for Domain Wall Motion in Antiferromagnetically Coupled Ferrimagnets, *Nat. Electron.* **2**, 389 (2019).
- [41] S. A. Siddiqui, J. Han, J. T. Finley, C. A. Ross, and L. Liu, Current-Induced Domain Wall Motion in a Compensated Ferrimagnet, *Phys. Rev. Lett.* **121**, 057701 (2018).
- [42] C. Sürgers, G. Fischer, P. Winkel, and H. v. Löhneysen, Large Topological Hall Effect in the Non-Collinear Phase of an Antiferromagnet, *Nat. Commun.* **5**, 8 (2014).
- [43] H.-J. Park, Y. Jeong, S.-H. Oh, G. Go, J. H. Oh, K.-W. Kim, H.-W. Lee, and K.-J. Lee, Numerical Computation of Spin-Transfer Torques for Antiferromagnetic Domain Walls, *Phys. Rev. B* **101**, 144431 (2020).
- [44] T. Okuno, Magnetic Dynamics in Antiferromagnetically-

- Coupled Ferrimagnets: The Role of Angular Momentum, *Springer Theses, Singapore* (2020).
- [45] W. Yu, J. Lan, and J. Xiao, Polarization-Selective Spin Wave Driven Domain-Wall Motion in Antiferromagnets, *Phys. Rev. B* **98**, 144422 (2018).
- [46] S. Dasgupta and J. Zou, Zeeman Term for the Néel Vector in a Two Sublattice Antiferromagnet, *Phys. Rev. B* **104**, 064415 (2021).
- [47] K.-J. Kim, S. K. Kim, Y. Hirata, S.-H. Oh, T. Tono, D.-H. Kim, T. Okuno, W. S. Ham, S. Kim, G. Go, Y. Tserkovnyak, A. Tsukamoto, T. Moriyama, K.-J. Lee, and T. Ono, Fast Domain Wall Motion in the Vicinity of the Angular Momentum Compensation Temperature of Ferrimagnets, *Nat. Mater.* **16**, 1187 (2017).
- [48] L. Caretta, S.-H. Oh, T. Fakhru, D.-K. Lee, B. H. Lee, S. K. Kim, C. A. Ross, K.-J. Lee, and G. S. D. Beach, Relativistic Kinematics of a Magnetic Soliton, *Science* **370**, 1438 (2020).
- [49] R. Cheng and Q. Niu, Electron Dynamics in Slowly Varying Antiferromagnetic Texture, *Phys. Rev. B* **86**, 245118 (2012).
- [50] R. Mondal and A. Kamra, Spin Pumping at Terahertz Nutation Resonances, *Phys. Rev. B* **104**, 214426 (2021).
- [51] G. Pacchioni, The Heat Is On, *Nat. Rev. Mater.* **5**, 868 (2020).
- [52] X. Yu, F. Kagawa, S. Seki, M. Kubota, J. Masell, F. S. Yasin, K. Nakajima, M. Nakamura, M. Kawasaki, N. Nagaoza, and Y. Tokura, Real-Space Observations of 60-Nm Skyrmion Dynamics in an Insulating Magnet under Low Heat Flow, *Nat. Commun.* **12**, 5079 (2021).
- [53] W. Jiang, P. Upadhyaya, Y. Fan, J. Zhao, M. Wang, L.-T. Chang, M. Lang, K. L. Wong, M. Lewis, Y.-T. Lin, J. Tang, S. Cherepov, X. Zhou, Y. Tserkovnyak, R. N. Schwartz, and K. L. Wang, Direct Imaging of Thermally Driven Domain Wall Motion in Magnetic Insulators, *Phys. Rev. Lett.* **110**, 177202 (2013).
- [54] R. Tolley, T. Liu, Y. Xu, S. Le Gall, M. Gottwald, T. Hauet, M. Hehn, F. Montaigne, E. E. Fullerton, and S. Mangin, Generation and Manipulation of Domain Walls Using a Thermal Gradient in a Ferrimagnetic TbCo Wire, *Appl. Phys. Lett.* **106**, 242403 (2015).
- [55] J. Torrejon, G. Malinowski, M. Pelloux, R. Weil, A. Thiaville, J. Curiale, D. Lacour, F. Montaigne, and M. Hehn, Unidirectional Thermal Effects in Current-Induced Domain Wall Motion, *Phys. Rev. Lett.* **109**, 106601 (2012).
- [56] G. Qin, X. Zhang, R. Zhang, K. Pei, C. Yang, C. Xu, Y. Zhou, Y. Wu, H. Du, and R. Che, Dynamics of Magnetic Skyrmions Driven by a Temperature Gradient in a Chiral Magnet FeGe, *Phys. Rev. B* **106**, 024415 (2022).
- [57] Y. A. Shokr, O. Sandig, M. Erkovan, B. Zhang, M. Bernien, A. A. Ünal, F. Kronast, U. Parlak, J. Vogel, and W. Kuch, Steering of Magnetic Domain Walls by Single Ultrashort Laser Pulses, *Phys. Rev. B* **99**, 214404 (2019).
- [58] S. U. Jen and L. Berger, Thermal Domain Drag Effect in Amorphous Ferromagnetic Materials. II. Experiments, *J. Appl. Phys.* **59**, 1285 (1986).
- [59] P. Yan, X. S. Wang, and X. R. Wang, All-Magnonic Spin-Transfer Torque and Domain Wall Propagation, *Phys. Rev. Lett.* **107**, 177207 (2011).
- [60] F. Schlickeiser, U. Ritzmann, D. Hinzke, and U. Nowak, Role of Entropy in Domain Wall Motion in Thermal Gradients, *Phys. Rev. Lett.* **113**, 097201 (2014).
- [61] X.-G. Wang, L. Chotorlishvili, G.-H. Guo, A. Sukhov, V. Dugaev, J. Barnaś, and J. Berakdar, Thermally Induced Magnonic Spin Current, Thermomagnonic Torques, and Domain-Wall Dynamics in the Presence of Dzyaloshinskii-Moriya Interaction, *Phys. Rev. B* **94**, 104410 (2016).
- [62] A. Sukhov, L. Chotorlishvili, A. Ernst, X. Zubizarreta, S. Ostianin, I. Mertig, E. K. U. Gross, and J. Berakdar, Swift Thermal Steering of Domain Walls in Ferromagnetic MnBi Stripes, *Sci. Rep.* **6**, 24411 (2016).
- [63] A. Donges, N. Grimm, F. Jakobs, S. Selzer, U. Ritzmann, U. Atxitia, and U. Nowak, Unveiling Domain Wall Dynamics of Ferrimagnets in Thermal Magnon Currents: Competition of Angular Momentum Transfer and Entropic Torque, *Phys. Rev. Research* **2**, 013293 (2020).
- [64] D. Hinzke and U. Nowak, Domain Wall Motion by the Magnonic Spin Seebeck Effect, *Phys. Rev. Lett.* **107**, 027205 (2011).
- [65] S. K. Kim and Y. Tserkovnyak, Landau-Lifshitz Theory of Thermomagnonic Torque, *Phys. Rev. B* **92**, 020410 (2015).
- [66] S. Selzer, U. Atxitia, U. Ritzmann, D. Hinzke, and U. Nowak, Inertia-Free Thermally Driven Domain-Wall Motion in Antiferromagnets, *Phys. Rev. Lett.* **117**, 107201 (2016).
- [67] X. S. Wang and X. R. Wang, Thermodynamic Theory for Thermal-Gradient-Driven Domain-Wall Motion, *Phys. Rev. B* **90**, 014414 (2014).
- [68] P. Yan, Y. Cao, and J. Sinova, Thermodynamic Magnon Recoil for Domain Wall Motion, *Phys. Rev. B* **92**, 100408 (2015).
- [69] Y. Wang, T. Shimada, J. Wang, T. Kitamura, and H. Hirakata, The Rectilinear Motion of the Individual Asymmetrical Skyrmion Driven by Temperature Gradients, *Acta Mater.* **117** 383 (2021).
- [70] I. O. Gorshkov, R. V. Gorev, M. V. Sapozhnikov, and O. G. Udalov, DMI-Gradient-Driven Skyrmion Motion, *ACS Appl. Electron. Mater.* **acsaelm.2c00404** (2022).
- [71] K. V. Yershov, V. P. Kravchuk, D. D. Sheka, J. van den Brink, and A. Saxena, Domain Wall Diode Based on Functionally Graded Dzyaloshinskii-Moriya Interaction, *Appl. Phys. Lett.* **116**, 222406 (2020).
- [72] L. Shen, J. Xia, G. Zhao, X. Zhang, M. Ezawa, O. A. Tretiakov, X. Liu, and Y. Zhou, Dynamics of the Antiferromagnetic Skyrmion Induced by a Magnetic Anisotropy Gradient, *Phys. Rev. B* **98**, 134448 (2018).
- [73] R. Tomasello, S. Komineas, G. Siracusano, M. Carpentieri, and G. Finocchio, Chiral Skyrmions in an Anisotropy Gradient, *Phys. Rev. B* **98**, 024421 (2018).
- [74] S. Moretti, V. Raposo, E. Martinez, and L. Lopez-Diaz, Domain Wall Motion by Localized Temperature Gradients, *Phys. Rev. B* **95**, 064419 (2017).
- [75] S. K. Kim, K. Nakata, D. Loss, and Y. Tserkovnyak, Tunable Magnonic Thermal Hall Effect in Skyrmion Crystal Phases of Ferrimagnets, *Phys. Rev. Lett.* **122**, 057204 (2019).
- [76] A. A. Kovalev, Skyrmionic Spin Seebeck Effect via Dissipative Thermomagnonic Torques, *Phys. Rev. B* **89**, 241101 (2014).
- [77] C. Bayer, H. Schultheiss, B. Hillebrands, and R. Stamps, Phase Shift of Spin Waves Traveling through a 180/Spl Deg/ Bloch-domain Wall, *IEEE Trans. Magn.* **41**, 3094 (2005).
- [78] R. Hertel, W. Wulfhekel, and J. Kirschner, Domain-Wall Induced Phase Shifts in Spin Waves, *Phys. Rev. Lett.* **93**, 257202 (2004).
- [79] Z.-X. Zhao, P.-B. He, M.-Q. Cai, and Z.-D. Li, Spin Waves and Transverse Domain Walls Driven by Spin Waves: Role of Damping, *Chin. Phys. B* **29**, 077502 (2020).
- [80] N. Kiriushcheva and S. Kuzmin, Scattering of a Gaussian Wave Packet by a Reflectionless Potential, *Am. J. Phys.* **66**, 867 (1998).
- [81] J.-S. Kim, M. Stärk, M. Kläui, J. Yoon, C.-Y. You, L. Lopez-Diaz, and E. Martinez, Interaction between Propagating Spin Waves and Domain Walls on a Ferromagnetic Nanowire, *Phys. Rev. B* **85**, 174428 (2012).
- [82] A. Ross, R. Lebrun, O. Gomonay, D. A. Grave, A. Kay, L. Baldrati, S. Becker, A. Qaiumzadeh, C. Ulloa, G. Jakob, F. Kronast, J. Sinova, R. Duine, A. Brataas, A. Rothschild, and M. Kläui, Propagation Length of Antiferromagnetic Magnons Governed by Domain Configurations, *Nano Lett.* **20**, 306 (2020).
- [83] A. Qaiumzadeh, L. A. Kristiansen, and A. Brataas, Controlling Chiral Domain Walls in Antiferromagnets Using Spin-Wave Helicity, *Phys. Rev. B* **97**, 020402 (2018).
- [84] S. J. Hämäläinen, M. Madami, H. Qin, G. Gubbiotti, and S. van Dijken, Control of Spin-Wave Transmission by a Programmable Domain Wall, *Nat. Commun.* **9**, 4853 (2018).
- [85] L.-J. Chang, Y.-F. Liu, M.-Y. Kao, L.-Z. Tsai, J.-Z. Liang, and S.-F. Lee, Ferromagnetic Domain Walls as Spin Wave Filters and the Interplay between Domain Walls and Spin Waves, *Sci. Rep.* **8**, 3910 (2018).

- [86] J. Lan, W. Yu, and J. Xiao, Antiferromagnetic Domain Wall as Spin Wave Polarizer and Retarder, *Nat. Commun.* **8**, 178 (2017).
- [87] P. Borys, F. Garcia-Sanchez, J.-V. Kim, and R. L. Stamps, Spin-Wave Eigenmodes of Dzyaloshinskii Domain Walls, *Adv. Electron. Mater.* **2**, 1500202 (2016).
- [88] W. Wang, M. Albert, M. Beg, M.-A. Bisotti, D. Chernyshenko, D. Cortés-Ortuño, I. Hawke, and H. Fangohr, Magnon-Driven Domain-Wall Motion with the Dzyaloshinskii-Moriya Interaction, *Phys. Rev. Lett.* **114**, 087203 (2015).
- [89] S. Schroeter and M. Garst, Scattering of High-Energy Magnons off a Magnetic Skyrmion, *Low Temp. Phys.* **41**, 817 (2015).
- [90] P. Pirro, T. Koyama, T. Brächer, T. Sebastian, B. Leven, and B. Hillebrands, Experimental Observation of the Interaction of Propagating Spin Waves with Néel Domain Walls in a Landau Domain Structure, *Appl. Phys. Lett.* **106**, 232405 (2015).
- [91] J. Iwasaki, A. J. Beekman, and N. Nagaosa, Theory of Magnon-Skyrmion Scattering in Chiral Magnets, *Phys. Rev. B* **89**, 064412 (2014).
- [92] H. Hata, T. Taniguchi, H.-W. Lee, T. Moriyama, and T. Ono, Spin-Wave-Induced Domain Wall Motion in Perpendicularly Magnetized System, *Appl. Phys. Express* **7**, 033001 (2014).
- [93] M. M. Bogdan and O. V. Charkina, Spin Waves in Easy-Axis Antiferromagnets with Precessing Domain Walls, *Low Temp. Phys.* **40**, 84 (2014).
- [94] X.-G. Wang, G.-H. Guo, G.-F. Zhang, Y.-Z. Nie, and Q.-L. Xia, Spin-Wave Resonance Reflection and Spin-Wave Induced Domain Wall Displacement, *J. Appl. Phys.* **113**, 213904 (2013).
- [95] X.-g. Wang, G.-h. Guo, G.-f. Zhang, Y.-z. Nie, and Q.-l. Xia, An Analytical Approach to the Interaction of a Propagating Spin Wave and a Bloch Wall, *Appl. Phys. Lett.* **102**, 132401 (2013).
- [96] D. Wang, X.-g. Wang, and G.-h. Guo, Magnonic Momentum Transfer Force on Domain Walls Confined in Space, *Europhys. Lett.* **101**, 27007 (2013).
- [97] X.-g. Wang, G.-h. Guo, Y.-z. Nie, G.-f. Zhang, and Z.-x. Li, Domain Wall Motion Induced by the Magnonic Spin Current, *Phys. Rev. B* **86**, 054445 (2012).
- [98] S. Macke and D. Goll, Transmission and Reflection of Spin Waves in the Presence of Néel Walls, *J. Phys.: Conf. Ser.* **200**, 042015 (2010).
- [99] S. Yuan, H. De Raedt, and S. Miyashita, Quantum Dynamics of Spin Wave Propagation through Domain Walls, *J. Phys. Soc. Jpn.* **75**, 084703 (2006).
- [100] S. H. Liu, Spin Waves in Static Non-Periodic Magnetic Structures, *J. Magn. Magn. Mater.* **12**, 262 (1979).
- [101] M. Mochizuki, X. Z. Yu, S. Seki, N. Kanazawa, W. Koshiba, J. Zang, M. Mostovoy, Y. Tokura, and N. Nagaosa, Thermally Driven Ratchet Motion of a Skyrmion Microcrystal and Topological Magnon Hall Effect, *Nat. Mater.* **13**, 241 (2014).
- [102] P. Shen, Y. Tserkovnyak, and S. K. Kim, Driving a Magnetized Domain Wall in an Antiferromagnet by Magnons, *J. Appl. Phys.* **127**, 223905 (2020).
- [103] C. Schütte and M. Garst, Magnon-Skyrmion Scattering in Chiral Magnets, *Phys. Rev. B* **90**, 094423 (2014).
- [104] V. Laliena, A. Athanasopoulos, and J. Campo, Scattering of Spin Waves by a Bloch Domain Wall: Effect of the Dipolar Interaction, *arXiv:2203.11140* (2022).
- [105] W. P. Sterk, H. Y. Yuan, A. Rückriegel, B. Z. Rameshti, and R. A. Duine, Green's Function Formalism for Nonlocal Elliptical Magnon Transport, *Phys. Rev. B* **104**, 174404 (2021).
- [106] E. Faridi, S. K. Kim, and G. Vignale, Atomic-Scale Spin-Wave Polarizer Based on a Sharp Antiferromagnetic Domain Wall, *arXiv:2203.01453* (2022).
- [107] M. W. Daniels, W. Yu, R. Cheng, J. Xiao, and D. Xiao, Topological Spin Hall Effects and Tunable Skyrmion Hall Effects in Uniaxial Antiferromagnetic Insulators, *Phys. Rev. B* **99**, 224433 (2019).
- [108] G. Zhang, Y. Tian, Y. Deng, D. Jiang, and S. Deng, Spin-Wave-Driven Skyrmion Motion in Magnetic Nanostrip, *J. Nanotechnol.* **2018**, 1 (2018).
- [109] M. Shen, Y. Zhang, J. Ou-Yang, X. Yang, and L. You, Motion of a Skyrmionium Driven by Spin Wave, *Appl. Phys. Lett.* **112**, 062403 (2018).
- [110] W. Kim and S. K. Kim, Interaction of Gapless Spin Waves and a Domain Wall in an Easy-Cone Ferromagnet, *arXiv:2211.03331* (2022).
- [111] N. N. Dadoenkova, Y. S. Dadoenkova, I. L. Lyubchanskii, M. Krawczyk, and K. Y. Guslienko, Inelastic Spin-Wave Scattering by Bloch Domain Wall Flexure Oscillations, *Phys. Status Solidi RRL* **13**, 1800589 (2019).
- [112] A. Janutka, Resonance of Spin Waves and Domain-Wall Excitations in Ferromagnetic Stripes, *IEEE Magn. Lett.* **4**, 4000104 (2013).
- [113] S.-M. Seo, H.-W. Lee, H. Kohno, and K.-J. Lee, Magnetic Vortex Wall Motion Driven by Spin Waves, *Appl. Phys. Lett.* **98**, 012514 (2011).
- [114] D.-S. Han, S.-K. Kim, J.-Y. Lee, S. J. Hermsdoerfer, H. Schultheiss, B. Leven, and B. Hillebrands, Magnetic Domain-Wall Motion by Propagating Spin Waves, *Appl. Phys. Lett.* **94**, 112502 (2009).
- [115] C. Jin, S. Li, H. Zhang, R. Wang, J. Wang, R. Lian, P. Gong, and X. Shi, Spin-Wave Modes of Elliptical Skyrmions in Magnetic Nanodots, *New J. Phys.* **24**, 043005 (2022).
- [116] P. Gruszecki and J. Kisielewski, Influence of Dzyaloshinskii-Moriya Interaction and Perpendicular Anisotropy on Spin Waves Propagation in Stripe Domain Patterns and Spin Spirals, *Research Square* (2022).
- [117] Z. Hu, Y. Shao, V. Lopez-Dominguez, and P. K. Amiri, Micromagnetic Investigation of a Voltage-Controlled Skyrmionic Magnon Switch, *Phys. Rev. Applied* **17**, 9 (2022).
- [118] J. Lan and J. Xiao, Skew Scattering and Side Jump of Spin Wave across Magnetic Texture, *Phys. Rev. B* **103**, 054428 (2021).
- [119] Y. Liu, T. T. Liu, Z. Jin, Z. P. Hou, D. Y. Chen, Z. Fan, M. Zeng, X. B. Lu, X. S. Gao, M. H. Qin, and J.-M. Liu, Spin-Wave-Driven Skyrmion Dynamics in Ferrimagnets: Effect of Net Angular Momentum, *Phys. Rev. B* **106** (2022).
- [120] Z. Wang, W. Bao, Y. Cao, and P. Yan, All-Magnonic Stern-Gerlach Effect in Antiferromagnets, *Appl. Phys. Lett.* **120**, 242403 (2022).
- [121] X. Zhang, Y. Zhang, S. Okamoto, and D. Xiao, Thermal Hall Effect Induced by Magnon-Phonon Interactions, *Phys. Rev. Lett.* **123**, 6 (2019).
- [122] W. Yu, J. Lan, and J. Xiao, Magnetic Logic Gate Based on Polarized Spin Waves, *Phys. Rev. Applied* **13**, 024055 (2020).
- [123] F. Ye and J. Lan, Magnetically Switchable Spin-Wave Retarder with 90° Antiferromagnetic Domain Wall, *Phys. Rev. B* **104**, 6 (2021).
- [124] W. Yu, J. Lan, R. Wu, and J. Xiao, Magnetic Snell's Law and Spin-Wave Fiber with Dzyaloshinskii-Moriya Interaction, *Phys. Rev. B* **94**, 140410 (2016).
- [125] K.-W. Moon, B. Sun Chun, W. Kim, and C. Hwang, Control of Domain Wall Motion by Interference of Spin Wave, *J. Appl. Phys.* **114**, 123908 (2013).
- [126] V. Laliena and J. Campo, Magnonic Goos-Hänchen Effect Induced by 1D Solitons, *Adv. Electron. Mater.* **8**, 2100782 (2022).
- [127] Z. Wang, Y. Cao, and P. Yan, Goos-Hänchen Effect of Spin Waves at Heterochiral Interfaces, *Phys. Rev. B* **100**, 6 (2019).
- [128] W. Bao, Z. Wang, Y. Cao, and P. Yan, Off-Axial Focusing of a Spin-Wave Lens in the Presence of Dzyaloshinskii-Moriya Interaction, *Phys. Rev. B* **102**, 014423 (2020).
- [129] F. Schlickeiser, U. Atxitia, S. Wienholdt, D. Hinzke, O. Chubykalo-Fesenko, and U. Nowak, Temperature Dependence of the Frequencies and Effective Damping Parameters of Ferrimagnetic Resonance, *Phys. Rev. B* **86**, 214416 (2012).
- [130] C. D. Stanciu, A. V. Kimel, F. Hansteen, A. Tsukamoto, A. Itoh, A. Kirilyuk, and Th. Rasing, Ultrafast Spin Dynamics across Compensation Points in Ferrimagnetic GdFeCo : The Role of Angular Momentum Compensation, *Phys. Rev. B* **73**, 220402 (2006).

- [131] M. Binder, A. Weber, O. Mosendz, G. Woltersdorf, M. Izquierdo, I. Neudecker, J. R. Dahn, T. D. Hatchard, J.-U. Thiele, C. H. Back, and M. R. Scheinfein, Magnetization Dynamics of the Ferrimagnet CoGd near the Compensation of Magnetization and Angular Momentum, *Phys. Rev. B* **74**, 134404 (2006).
- [132] L. Caretta, M. Mann, F. Büttner, K. Ueda, B. Pfau, C. M. Günther, P. Hessing, A. Churikova, C. Klose, M. Schneider, D. Engel, C. Marcus, D. Bono, K. Bagschik, S. Eisebitt, and G. S. D. Beach, Fast Current-Driven Domain Walls and Small Skyrmions in a Compensated Ferrimagnet, *Nat. Nanotechnol.* **13**, 1154 (2018).
- [133] S. K. Kim, Y. Tserkovnyak, and O. Tchernyshyov, Propulsion of a Domain Wall in an Antiferromagnet by Magnons, *Phys. Rev. B* **90**, 104406 (2014).
- [134] G. Tatara and H. Kohno, Theory of Current-Driven Domain Wall Motion: Spin Transfer versus Momentum Transfer, *Phys. Rev. Lett.* **92**, 086601 (2004).
- [135] C. Gong, Y. Zhou, and G. Zhao, Dynamics of Magnetic Skyrmions under Temperature Gradients, *Appl. Phys. Lett.* **120**, 052402 (2022).
- [136] A. Abbot, J. Weston, X. Waintal, and A. Manchon, Cooperative Charge Pumping and Enhanced Skyrmion Mobility, *Phys. Rev. Lett.* **121**, 257203 (2018).
- [137] G. Tatara, Thermal Vector Potential Theory of Magnon-Driven Magnetization Dynamics, *Phys. Rev. B* **92**, 064405 (2015).
- [138] L. Shen, J. Xia, X. Zhang, M. Ezawa, O. A. Tretiakov, X. Liu, G. Zhao, and Y. Zhou, Current-Induced Dynamics and Chaos of Antiferromagnetic Bimerons, *Phys. Rev. Lett.* **124**, 037202 (2020).
- [139] S. Woo and G. S. D. Beach, Control of Propagating Spin-Wave Attenuation by the Spin-Hall Effect, *J. Appl. Phys.* **122**, 093901 (2017).
- [140] S. K. Kim, O. Tchernyshyov, and Y. Tserkovnyak, Thermophoresis of an Antiferromagnetic Soliton, *Phys. Rev. B* **92**, 020402 (2015).
- [141] E. M. Lifshitz and L. D. Landau, Course of Theoretical Physics: Vol. 4, Quantum Electrodynamics, 2nd Edition, *Butterworth-Heinemann* (1982).
- [142] X.-G. Wen, *Quantum Field Theory of Many-Body Systems: From the Origin of Sound to an Origin of Light and Electrons*, Oxford Graduate Texts (Oxford University Press, Oxford, 2010).
- [143] O. Tchernyshyov, Conserved Momenta of a Ferromagnetic Soliton, *Ann. Phys.* **363**, 98 (2015).
- [144] P. Nieves, D. Serantes, and O. Chubykalo-Fesenko, Self-Consistent Description of Spin-Phonon Dynamics in Ferromagnets, *Phys. Rev. B* **94**, 014409 (2016).
- [145] S. K. Kim, O. Tchernyshyov, V. Galitski, and Y. Tserkovnyak, Magnon-Induced Non-Markovian Friction of a Domain Wall in a Ferromagnet, *Phys. Rev. B* **97**, 174433 (2018).
- [146] C. A. Akosa, I. M. Miron, G. Gaudin, and A. Manchon, Phenomenology of Chiral Damping in Noncentrosymmetric Magnets, *Phys. Rev. B* **93**, 5 (2016).
- [147] C. A. Akosa, P. B. Ndiaye, and A. Manchon, Intrinsic Nonadiabatic Topological Torque in Magnetic Skyrmions and Vortices, *Phys. Rev. B* **95**, 054434 (2017).
- [148] K. M. D. Hals, A. K. Nguyen, and A. Brataas, Intrinsic Coupling between Current and Domain Wall Motion in (Ga,Mn)As, *Phys. Rev. Lett.* **102**, 256601 (2009).
- [149] M. Weissenhofer, L. Rózsa, and U. Nowak, Skyrmion Dynamics at Finite Temperatures: Beyond Thiele's Equation, *Phys. Rev. Lett.* **127**, 047203 (2021).
- [150] K.-J. Kim, R. Hiramatsu, T. Koyama, K. Ueda, Y. Yoshimura, D. Chiba, K. Kobayashi, Y. Nakatani, S. Fukami, M. Yamamoto, H. Ohno, H. Kohno, G. Tatara, and T. Ono, Two-Barrier Stability That Allows Low-Power Operation in Current-Induced Domain-Wall Motion, *Nat. Commun.* **4**, 2011 (2013).
- [151] H. Kohno, G. Tatara, and J. Shibata, Microscopic Calculation of Spin Torques in Disordered Ferromagnets, *J. Phys. Soc. Jpn.* **75**, 113706 (2006).
- [152] K. Litzius, I. Lemesh, B. Krüger, P. Bassirian, L. Caretta, K. Richter, F. Büttner, K. Sato, O. A. Tretiakov, J. Förster, R. M. Reeve, M. Weigand, I. Bykova, H. Stoll, G. Schütz, G. S. D. Beach, and M. Kläui, Skyrmion Hall Effect Revealed by Direct Time-Resolved X-ray Microscopy, *Nat. Phys.* **13**, 170 (2017).
- [153] A. Mougin, M. Cormier, J. P. Adam, P. J. Metaxas, and J. Ferré, Domain Wall Mobility, Stability and Walker Breakdown in Magnetic Nanowires, *Europhys. Lett.* **78**, 57007 (2007).
- [154] H. Kohno and J. Shibata, Gauge Field Formulation of Adiabatic Spin Torques, *J. Phys. Soc. Jpn.* **76**, 063710 (2007).
- [155] R. Gruber, J. Zázvorka, M. A. Brems, D. R. Rodrigues, T. Dohi, N. Kerber, B. Seng, M. Vafaee, K. Everschor-Sitte, P. Virnau, and M. Kläui, Skyrmion Pinning Energetics in Thin Film Systems, *Nat. Commun.* **13**, 3144 (2022).
- [156] L. Berges, E. Haltz, S. Panigrahy, S. Mallick, R. Weil, S. Rothart, A. Mougin, and J. Sampaio, Size-Dependent Mobility of Skyrmions beyond Pinning in Ferrimagnetic GdCo Thin Films, *Phys. Rev. B* **106**, 144408 (2022).
- [157] F. J. Buijnsters, A. Fassolino, and M. I. Katsnelson, Motion of Domain Walls and the Dynamics of Kinks in the Magnetic Peierls Potential, *Phys. Rev. Lett.* **113**, 217202 (2014).
- [158] E. Jué, C. K. Safeer, M. Drouard, A. Lopez, P. Balint, L. Budapesteanu, O. Boulle, S. Auffret, A. Schuhl, A. Manchon, I. M. Miron, and G. Gaudin, Chiral Damping of Magnetic Domain Walls, *Nat. Mater.* **15**, 272 (2016).
- [159] L. D. Landau and E. M. Lifshits, Course of Theoretical Physics: Vol. 3, Quantum Mechanics: Non-Relativistic Theory, 3rd Edition, *Butterworth-Heinemann* (1981).
- [160] G. Su, B. Chen, and M. Ge, Temperature Dependence of the Coercivity for Some Intermetallic Magnetic Particles at Low Temperatures, *Phys. Status Solidi B* **181**, K33 (1994).
- [161] A. Derras-Chouk, E. M. Chudnovsky, and D. A. Garanin, Dynamics of the Collapse of a Ferromagnetic Skyrmion in a Centrosymmetric Lattice, *Phys. Rev. B* **105**, 134432 (2022).
- [162] S. Dasgupta and O. Tchernyshyov, Energy-Momentum Tensor of a Ferromagnet, *Phys. Rev. B* **98**, 224401 (2018).
- [163] A. Thiaville, Y. Nakatani, J. Miltat, and Y. Suzuki, Micromagnetic Understanding of Current-Driven Domain Wall Motion in Patterned Nanowires, *Europhys. Lett.* **69**, 990 (2005).
- [164] V. Jeudy, A. Mougin, S. Bustingorry, W. Savero Torres, J. Gorchein, A. B. Kolton, A. Lemaître, and J.-P. Jamet, Universal Pinning Energy Barrier for Driven Domain Walls in Thin Ferromagnetic Films, *Phys. Rev. Lett.* **117**, 057201 (2016).
- [165] M. Eltschka, M. Wötzl, J. Rhensius, S. Krzyk, U. Nowak, M. Kläui, T. Kasama, R. E. Dunin-Borkowski, L. J. Heyderman, H. J. van Driel, and R. A. Duine, Nonadiabatic Spin Torque Investigated Using Thermally Activated Magnetic Domain Wall Dynamics, *Phys. Rev. Lett.* **105**, 056601 (2010).
- [166] D.-H. Kim, K.-W. Moon, S.-C. Yoo, B.-C. Min, K.-H. Shin, and S.-B. Choe, A Method for Compensating the Joule-Heating Effects in Current-Induced Domain Wall Motion, *IEEE Trans. Magn.* **49**, 3207 (2013).
- [167] K. Litzius, J. Leliaert, P. Bassirian, D. Rodrigues, S. Kromin, I. Lemesh, J. Zázvorka, K.-J. Lee, J. Mulkers, N. Kerber, D. Heinze, N. Keil, R. M. Reeve, M. Weigand, B. Van Waeyenberge, G. Schütz, K. Everschor-Sitte, G. S. D. Beach, and M. Kläui, The Role of Temperature and Drive Current in Skyrmion Dynamics, *Nat. Electron.* **3**, 30 (2020).
- [168] F. Freimuth, S. Blügel, and Y. Mokrousov, Direct and Inverse Spin-Orbit Torques, *Phys. Rev. B* **92**, 19 (2015).
- [169] C. Zhang, J. Wang, C. Jin, Z. Zeng, H. Xia, J. Wang, and Q. Liu, Spin Current Pumped by Confined Breathing Skyrmion, *New J. Phys.* **22**, 053029 (2020).
- [170] D. A. Reiss and P. W. Brouwer, Finite-Frequency Spin Conductance of the Interface between a Ferro- or Ferrimagnetic Insulator and a Normal Metal, *Phys. Rev. B* **106**, 144423 (2022).
- [171] G. E. W. Bauer, S. Bretzel, A. Brataas, and Y. Tserkovnyak, Nanoscale Magnetic Heat Pumps and Engines, *Phys. Rev. B* **81**, 11 (2010).
- [172] C. H. Wong, H. J. van Driel, R. Kittinaradorn, H. T. C. Stoof,

- and R. A. Duine, Spin Caloritronics in Noncondensed Bose Gases, *Phys. Rev. Lett.* **108**, 075301 (2012).
- [173] H.-T. Huang, M.-F. Lai, Y.-F. Hou, and Z.-H. Wei, Influence of Magnetic Domain Walls and Magnetic Field on the Thermal Conductivity of Magnetic Nanowires, *Nano Lett.* **15**, 2773 (2015).
- [174] O. Boulle, L. D. Buda-Prejbeanu, E. Jué, I. M. Miron, and G. Gaudin, Current Induced Domain Wall Dynamics in the Presence of Spin Orbit Torques, *J. Appl. Phys.* **115**, 17D502 (2014).
- [175] E. Saitoh, H. Miyajima, T. Yamaoka, and G. Tatara, Current-Induced Resonance and Mass Determination of a Single Magnetic Domain Wall, *Nature* **432**, 203 (2004).
- [176] G. Tatara and H. Fukuyama, Resistivity Due to a Domain Wall in Ferromagnetic Metal, *Phys. Rev. Lett.* **78**, 3773 (1997).
- [177] G. Tatara, Domain Wall Resistance Based on Landauer's Formula, *J. Phys. Soc. Jpn.* **69**, 2969 (2000).
- [178] GEN. TATARA, DOMAIN WALL RESISTIVITY BASED ON A LINEAR RESPONSE THEORY, *Int. J. Mod. Phys. B* **15**, 321 (2001).
- [179] M. E. Lucassen, C. H. Wong, R. A. Duine, and Y. Tserkovnyak, Spin-Transfer Mechanism for Magnon-Drag Thermopower, *Appl. Phys. Lett.* **99**, 262506 (2011).
- [180] Z. Y. Tian, Q. Y. Zhang, Y. W. Xiao, G. A. Gamage, F. Tian, S. Yue, V. G. Hadjiev, J. Bao, Z. Ren, E. Liang, and J. Zhao, Ultraweak Electron-Phonon Coupling Strength in Cubic Boron Arsenide Unveiled by Ultrafast Dynamics, *Phys. Rev. B* **105**, 11 (2022).
- [181] S. D. Brechet, F. A. Vetro, E. Papa, S. E. Barnes, and J.-P. Ansermet, Evidence for a Magnetic Seebeck Effect, *Phys. Rev. Lett.* **111**, 087205 (2013).
- [182] S. E. Nikitin, B. Fåk, K. W. Krämer, T. Fennell, B. Normand, A. M. Läuchli, and Ch. Rüegg, Thermal Evolution of Dirac Magnons in the Honeycomb Ferromagnet CrBr₃, *Phys. Rev. Lett.* **129**, 127201 (2022).
- [183] K. Cai, Z. Zhu, J. M. Lee, R. Mishra, L. Ren, S. D. Pollard, P. He, G. Liang, K. L. Teo, and H. Yang, Ultrafast and Energy-Efficient Spin–Orbit Torque Switching in Compensated Ferromagnets, *Nat. Electron.* **3**, 37 (2020).
- [184] R. Khoshlahni, A. Qaiumzadeh, A. Bergman, and A. Brataas, Ultrafast Generation and Dynamics of Isolated Skyrmions in Antiferromagnetic Insulators, *Phys. Rev. B* **99**, 054423 (2019).
- [185] S.-Z. Lin, C. D. Batista, C. Reichhardt, and A. Saxena, Ac Current Generation in Chiral Magnetic Insulators and Skyrmion Motion Induced by the Spin Seebeck Effect, *Phys. Rev. Lett.* **112**, 187203 (2014).
- [186] Y.-R. Wang, C. Yang, Z.-C. Wang, and G. Su, Domain-Wall Dynamics Driven by Thermal and Electrical Spin-Transfer Torque, *Phys. Rev. B* **106**, 054432 (2022).
- [187] E. Faridi, S. K. Kim, and G. Vignale, Atomic-Scale Spin-Wave Polarizer Based on a Sharp Antiferromagnetic Domain Wall, *Phys. Rev. B* **106**, 094411 (2022).
- [188] A. Thiaville, S. Rohart, É. Jué, V. Cros, and A. Fert, Dynamics of Dzyaloshinskii Domain Walls in Ultrathin Magnetic Films, *Europhys. Lett.* **100**, 57002 (2012).
- [189] O. A. Tretiakov and Ar. Abanov, Current Driven Magnetization Dynamics in Ferromagnetic Nanowires with a Dzyaloshinskii-Moriya Interaction, *Phys. Rev. Lett.* **105**, 157201 (2010).
- [190] J. Chen, J. Hu, and H. Yu, Chiral Emission of Exchange Spin Waves by Magnetic Skyrmions, *ACS Nano* **15**, 4372 (2021).
- [191] Y.-C. Liang, P.-B. He, M.-Q. Cai, and Z.-D. Li, Motion and Stability of Chiral Domain Walls Driven by Non-Gradient Spin Torques: Antiferromagnets and Ferromagnets Compared, *J. Magn. Magn. Mater.* **479**, 291 (2019).
- [192] J. Han, P. Zhang, J. T. Hou, S. A. Siddiqui, and L. Liu, Mutual Control of Coherent Spin Waves and Magnetic Domain Walls in a Magnonic Device, *Science* **366**, 1121 (2019).
- [193] L. Kong, X. Chen, W. Wang, D. Song, and H. Du, Dynamics of Interstitial Skyrmions in the Presence of Temperature Gradients, *Phys. Rev. B* **104**, 214407 (2021).
- [194] R. Knapman, D. R. Rodrigues, J. Masell, and K. Everschor-Sitte, Current-Induced H-shaped-skyrmion Creation and Their Dynamics in the Helical Phase, *J. Phys. D: Appl. Phys.* **54**, 404003 (2021).
- [195] O. Boulle, S. Rohart, L. D. Buda-Prejbeanu, E. Jué, I. M. Miron, S. Pizzini, J. Vogel, G. Gaudin, and A. Thiaville, Domain Wall Tilting in the Presence of the Dzyaloshinskii-Moriya Interaction in Out-of-Plane Magnetized Magnetic Nanotrails, *Phys. Rev. Lett.* **111**, 5 (2013).
- [196] T. Dohi, M. Weißhofer, N. Kerber, F. Kammerbauer, Y. Ge, K. Raab, J. Zázvorka, M.-A. Syskaki, A. Shahee, and M. Ruhwedel, Enhanced Thermally-Activated Skyrmion Diffusion in Synthetic Antiferromagnetic Systems with Tunable Effective Topological Charge, *arXiv:2206.00791* (2022).
- [197] S. Jen and L. Berger, Dragging of Stripe Domains by a Temperature Gradient in Metglas 2826 MB (Invited), *J. Appl. Phys.* **53**, 2298 (1982).
- [198] K. Tanabe, D. Chiba, J. Ohe, S. Kasai, H. Kohno, S. E. Barnes, S. Maekawa, K. Kobayashi, and T. Ono, Spin-Motive Force Due to a Gyrating Magnetic Vortex, *Nat. Commun.* **3**, 845 (2012).
- [199] M. Agrawal, V. I. Vasyuchka, A. A. Serga, A. D. Karenowska, G. A. Melkov, and B. Hillebrands, Direct Measurement of Magnon Temperature: New Insight into Magnon-Phonon Coupling in Magnetic Insulators, *Phys. Rev. Lett.* **111**, 107204 (2013).
- [200] T. An, V. I. Vasyuchka, K. Uchida, A. V. Chumak, K. Yamaguchi, K. Harii, J. Ohe, M. B. Jungfleisch, Y. Kajiwara, H. Adachi, B. Hillebrands, S. Maekawa, and E. Saitoh, Unidirectional Spin-Wave Heat Conveyer, *Nat. Mater.* **12**, 549 (2013).
- [201] P. Yan and G. E. W. Bauer, Magnon Mediated Domain Wall Heat Conductance in Ferromagnetic Wires, *IEEE Trans. Magn.* **49**, 3109 (2013).
- [202] S. Lee, K. Hippalgaonkar, F. Yang, J. Hong, C. Ko, J. Suh, K. Liu, K. Wang, J. J. Urban, X. Zhang, C. Dames, S. A. Hartnoll, O. Delaire, and J. Wu, Anomalously Low Electronic Thermal Conductivity in Metallic Vanadium Dioxide, *Science* **355**, 371 (2017).
- [203] L. Qiu and K. Shen, Tunable Spin-Wave Nonreciprocity in Synthetic Antiferromagnetic Domain Walls, *Phys. Rev. B* **105**, 094436 (2022).
- [204] B. Flebus, S. A. Bender, Y. Tserkovnyak, and R. A. Duine, Two-Fluid Theory for Spin Superfluidity in Magnetic Insulators, *Phys. Rev. Lett.* **116**, 117201 (2016).
- [205] S. R. Boona, S. J. Watzman, and J. P. Heremans, Research Update: Utilizing Magnetization Dynamics in Solid-State Thermal Energy Conversion, *APL Mater.* **4**, 104502 (2016).
- [206] T. Yamaguchi, H. Kohno, and R. A. Duine, Microscopic Theory of Magnon-Drag Electron Flow in Ferromagnetic Metals, *Phys. Rev. B* **99**, 094425 (2019).
- [207] D. Miura and A. Sakuma, Microscopic Theory of Magnon-Drag Thermoelectric Transport in Ferromagnetic Metals, *J. Phys. Soc. Jpn.* **81**, 113602 (2012).
- [208] E. LIU and S. ZHANG, Topologically Enhanced Zero-Field Transverse Nernstthermoelectric Effect in Magnetic Topological Semimetals (inChinese), *Sci. China-Phys. Mech. Astron.* **49**, 127001 (2019).
- [209] Y. Kasahara, T. Ohnishi, Y. Mizukami, O. Tanaka, S. Ma, K. Sugii, N. Kurita, H. Tanaka, J. Nasu, Y. Motome, T. Shibauchi, and Y. Matsuda, Majorana Quantization and Half-Integer Thermal Quantum Hall Effect in a Kitaev Spin Liquid, *Nature* **559**, 227 (2018).
- [210] P. Wei, J. Yang, L. Guo, S. Wang, L. Wu, X. Xu, W. Zhao, Q. Zhang, W. Zhang, M. S. Dresselhaus, and J. Yang, Minimum Thermal Conductivity in Weak Topological Insulators with Bismuth-Based Stack Structure, *Adv. Funct. Mater.* **26**, 5360 (2016).
- [211] J. Liang, L. Cheng, J. Zhang, H. Liu, and Z. Zhang, Maximizing the Thermoelectric Performance of Topological Insulator Bi₂Te₃films in the Few-Quintuple Layer Regime, *Nanoscale* **8**, 8855 (2016).

- [212] Y. Xu, Z. Gan, and S.-C. Zhang, Enhanced Thermoelectric Performance and Anomalous Seebeck Effects in Topological Insulators, *Phys. Rev. Lett.* **112**, 226801 (2014).
- [213] F. Zahid and R. Lake, Thermoelectric Properties of Bi₂Te₃ Atomic Quintuple Thin Films, *Appl. Phys. Lett.* **97**, 212102 (2010).
- [214] V. Goyal, D. Teweldebrhan, and A. A. Balandin, Mechanically-Exfoliated Stacks of Thin Films of Bi₂Te₃ Topological Insulators with Enhanced Thermoelectric Performance, *Appl. Phys. Lett.* **97**, 133117 (2010).
- [215] J. Ye, Y. B. Kim, A. J. Millis, B. I. Shraiman, P. Majumdar, and Z. Tešanović, Berry Phase Theory of the Anomalous Hall Effect: Application to Colossal Magnetoresistance Manganites, *Phys. Rev. Lett.* **83**, 3737 (1999).
- [216] K. Hamamoto, M. Ezawa, and N. Nagaosa, Quantized Topological Hall Effect in Skyrmion Crystal, *Phys. Rev. B* **92**, 115417 (2015).
- [217] Y. Wang, N. S. Rogado, R. J. Cava, and N. P. Ong, Spin Entropy as the Likely Source of Enhanced Thermopower in Na_xCo₂O₄, *Nature* **423**, 425 (2003).
- [218] J. Flipse, F. K. Dejene, D. Wagenaar, G. E. W. Bauer, J. B. Youssef, and B. J. van Wees, Observation of the Spin Peltier Effect for Magnetic Insulators, *Phys. Rev. Lett.* **113**, 027601 (2014).
- [219] S. A. Yang, G. S. D. Beach, C. Knutson, D. Xiao, Z. Zhang, M. Tsoi, Q. Niu, A. H. MacDonald, and J. L. Erskine, Topological Electromotive Force from Domain-Wall Dynamics in a Ferromagnet, *Phys. Rev. B* **82**, 054410 (2010).
- [220] Y. Yamane and J. Ieda, Skyrmion-Generated Spinmotive Forces in Inversion Broken Ferromagnets, *J. Magn. Magn. Mater.* **491**, 165550 (2019).
- [221] L. Šmejkal, Y. Mokrousov, B. Yan, and A. H. MacDonald, Topological Antiferromagnetic Spintronics, *Nat. Phys.* **14**, 242 (2018).
- [222] E. G. Tveten, T. Müller, J. Linder, and A. Brataas, Intrinsic Magnetization of Antiferromagnetic Textures, *Phys. Rev. B* **93**, 104408 (2016).
- [223] C. A. Akosa, O. A. Tretiakov, G. Tatara, and A. Manchon, Theory of the Topological Spin Hall Effect in Antiferromagnetic Skyrmions: Impact on Current-Induced Motion, *Phys. Rev. Lett.* **121**, 097204 (2018).
- [224] W. Feng, J.-P. Hanke, X. Zhou, G.-Y. Guo, S. Blügel, Y. Mokrousov, and Y. Yao, Topological Magneto-Optical Effects and Their Quantization in Noncoplanar Antiferromagnets, *Nat. Commun.* **11**, 118 (2020).
- [225] Z. Y. Chen, Z. R. Yan, M. H. Qin, and J.-M. Liu, Landau-Lifshitz-Bloch Equation for Domain Wall Motion in Antiferromagnets, *Phys. Rev. B* **99**, 214436 (2019).